Geological Society of America Bulletin

Deriving a long paleoseismic record from a shallow-water Holocene basin next to the Alpine fault, New Zealand

K.J. Clark, U.A. Cochran, K.R. Berryman, G. Biasi, P. Villamor, T. Bartholomew, N. Litchfield, D. Pantosti, S. Marco, R. Van Dissen, G. Turner and M. Hemphill-Haley

Geological Society of America Bulletin published online 22 February 2013;
doi: 10.1130/B30693.1

Notes

Geological Society of America Bulletin, published online on 22 February 2013 as doi:10.1130/B30693.1

Deriving a long paleoseismic record from a shallow-water Holocene basin next to the Alpine fault, New Zealand

K.J. Clark[1,†], U.A. Cochran[1], K.R. Berryman[1], G. Biasi[2], R. Langridge[1], P. Villamor[1], T. Bartholomew[3], N. Litchfield[1], D. Pantosti[4], S. Marco[5], R. Van Dissen[1], G. Turner[6], and M. Hemphill-Haley[7]

[1]*GNS Science, P.O. Box 30368, Lower Hutt, New Zealand*
[2]*Seismological Laboratory, MS-174, University of Nevada, Reno, Nevada 89557, USA*
[3]*School of Geography, Environment and Earth Sciences, Victoria University of Wellington, P.O. Box 600, Wellington, New Zealand*
[4]*Istituto Nazionale di Geofisica e Vulcanologia, Via di Vigna Murata 605, 00143 Rome, Italy*
[5]*Department of Geophysics and Planetary Sciences, Tel Aviv University, Tel Aviv 69978, Israel*
[6]*School of Chemical and Physical Sciences, Victoria University of Wellington, P.O. Box 600, Wellington, New Zealand*
[7]*Department of Geology, Humboldt State University, Arcata, California 95521, USA*

ABSTRACT

A sedimentary sequence that was highly sensitive to fault rupture–driven changes in water level and sediment supply has been used to extract a continuous record of 22 large earthquakes on the Alpine fault, the fastest-slipping fault in New Zealand. At Hokuri Creek, in South Westland, an 18 m thickness of Holocene sediments accumulated against the Alpine fault scarp from ca. A.D. 800 to 6000 B.C. We used geomorphological mapping, sedimentology, and paleoenvironmental reconstruction to investigate the relationship between these sediments and Alpine fault rupture. We found that repeated fault rupture is the most convincing mechanism for explaining all the features of the alternating peat and silt sedimentary sequence. Climate has contributed to sedimentation but is unlikely to be the driver of these cyclical changes in sediment type and paleoenvironment. Other nontectonic causes for the sedimentary alternations do not produce the incremental increase in basin accommodation space necessary to maintain the shallow-water environment for 6800 yr. Our detailed documentation of this near-fault sedimentary basin sequence highlights the advantages of extracting paleoearthquake records from such sites—the continuity of sedimentation, abundance of dateable material, and pristine preservation of older events.

INTRODUCTION

Records of large earthquakes spanning thousands of years are vital for quantifying seismic hazard because instrumental and historical records are rarely long enough to capture the natural variability in earthquake timing. Knowledge of the variability of earthquake recurrence on individual faults improves understanding of factors controlling or affecting the timing of earthquakes, such as strain accumulation, stress transfer, and interactions with other faults. Determining fault behavior over many seismic cycles enables selection of more appropriate seismic hazard models for quantification of earthquake hazard (e.g., Chui, 2009; Parsons, 2008).

Long on-fault (adjacent to surface faults) paleoseismic records are rare because the preservation of evidence for fault rupture requires a fine balance between sedimentation and fault slip. Ideally, sedimentation needs to be continuous but not at such a high rate that older sequences are buried at a depth out of reach by trenching or coring. Long on-fault paleoseismic records have been derived from extensive trenching (e.g., San Andreas fault—Scharer et al., 2010; Weldon et al., 2004; Hayward fault—Lienkaemper and Williams, 2007; Dead Sea fault—Ferry et al., 2011). These records make important contributions to understanding fault behavior but are hampered by breaks in the record (Scharer et al., 2010) or only capture 11–12 earthquakes (Ferry et al., 2011; Lienkaemper and Williams, 2007), when a greater number of earthquakes is preferred to test various fault behavior models.

Off-fault paleoseismic records can have the advantage of greater temporal continuity and can extend further back in time. For example, the seismite record within naturally exposed lake sediments along the Dead Sea Transform extends back 50,000 yr (Marco et al., 1996), and deep-sea turbidites represent 18 earthquakes at the Cascadia subduction zone (Goldfinger et al., 2003). However, off-fault paleoseismic evidence typically records large earthquakes in a given region and can rarely be unequivocally related to a single fault source. Thus, one cannot be certain if the numbers of earthquakes for a given fault are under- or overestimated.

A long paleoearthquake record for the Alpine fault in New Zealand has been obtained from an unusual sedimentary record (Berryman et al., 2012b). The record relies on natural exposures of a sequence of Holocene sediments on the downthrown side of the Alpine fault at Hokuri Creek. Sedimentation is recorded on only one side of the fault, so we refer to the Hokuri record as a "near-fault" record.

In this study, we present the lithofacies of the Hokuri sequence and use paleoenvironmental information to develop a depositional model dominated by cyclical hydrological and sedimentary changes. By integrating recent tectonic geomorphology and radiocarbon age data with the depositional model, we conclude that the most likely process driving the repeated sedimentary and hydrologic changes is surface

[†]E-mail: k.clark@gns.cri.nz

 doi: 10.1130/B30693.1; 15 figures; 2 tables; Data Repository item 2013133.

Geological Society of America Bulletin, published online on 22 February 2013 as doi:10.1130/B30693.1

rupture of the Alpine fault. Processes other than earthquakes that could have caused the observed stratigraphic changes are considered, as is the potential for under- or overrepresentation of paleoearthquakes. This inquisition is essential for ensuring the reliability of the Hokuri paleoearthquake record, one of the longest continuous large earthquake records globally.

SETTING OF THE ALPINE FAULT AND HOKURI CREEK SITE

New Zealand's Alpine fault is a major plate-boundary fault accommodating two thirds to three quarters of the motion between the Australian and Pacific plates (Fig. 1A; Norris and Cooper, 2001; Sutherland et al., 2006). With a strike-slip rate of 23–31 mm/yr (Barnes, 2009; Norris and Cooper, 2007; Sutherland et al., 2006), it is one of the fastest-slipping faults in the world and is considered to rupture in large to great earthquakes (Sutherland et al., 2007). The Alpine fault has a remarkably straight 400 km onshore trace at the western edge of the Southern Alps (Fig. 1A; Berryman et al., 1992; Norris

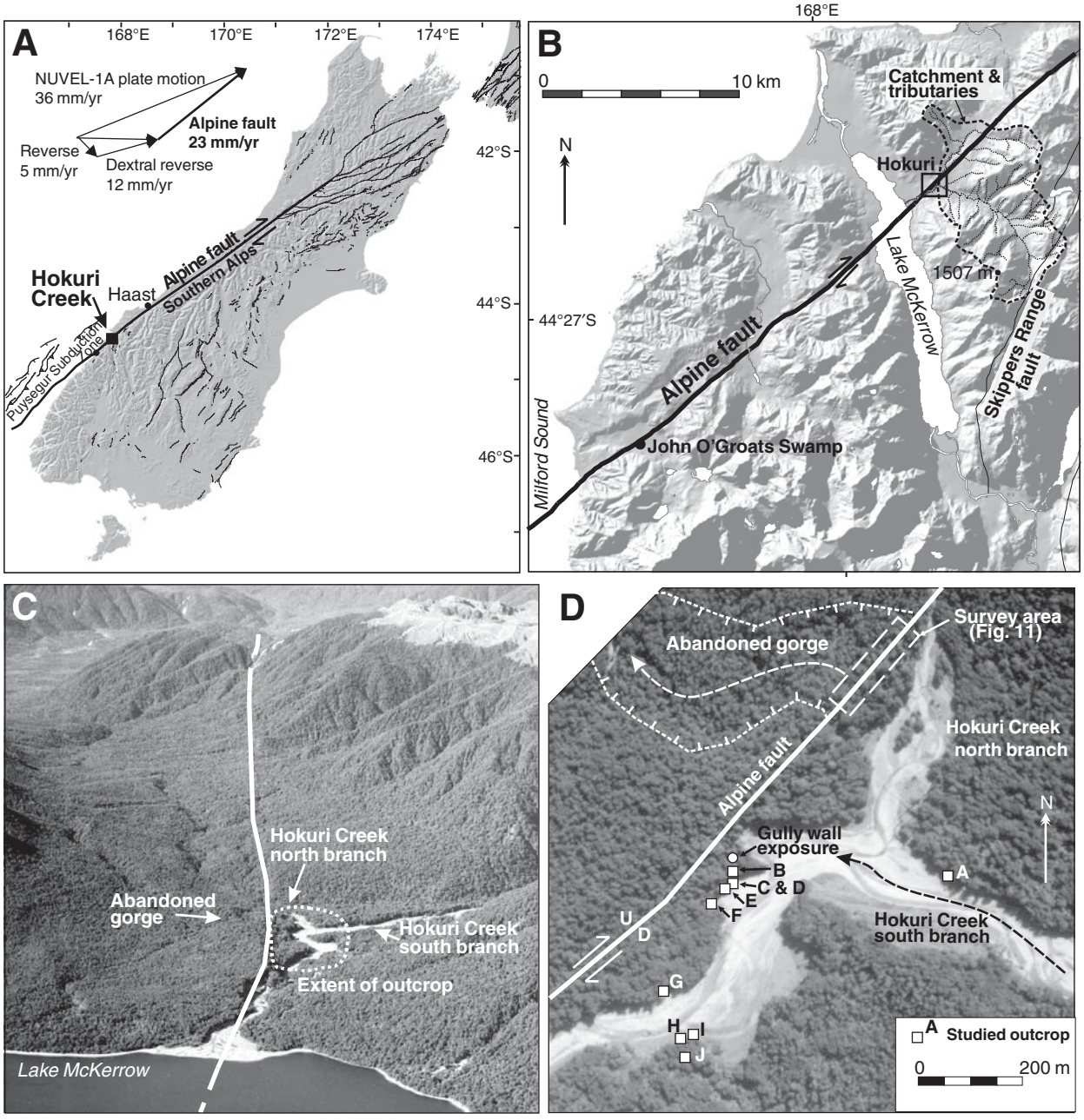

Figure 1. (A) Active faults of the South Island, New Zealand. Data sources: New Zealand Active Faults Database (http://data.gns.cri.nz/af/), Barnes (2009) and Sutherland et al. (2006). (B) Shaded digital elevation model of the southern onshore section of the Alpine fault showing location of the Hokuri Creek study area and John O'Groats swamp. (C) Oblique aerial photograph of the Hokuri area, photo looking to the northeast along the Alpine fault (photo by Lloyd Homer). (D) Vertical aerial photograph of the Hokuri study region showing the major geomorphic features and the studied outcrop locations.

Geological Society of America Bulletin, published online on 22 February 2013 as doi:10.1130/B30693.1

and Cooper, 2001, 2007). At 44.53°S (at Milford Sound), the Alpine fault crosses the shore and continues for a further 230 km until terminating at the Puysegur Trench (Barnes et al., 2005). At the surface, the fault is generally manifest as a single trace with few large (>3 km) stepovers or areas of distributed deformation. At a local scale (<~3 km), there are structural complexities along the Alpine fault with varying amounts of reverse and strike-slip motion depending on fault orientation (Norris and Cooper, 1995, 1997). Due to the absence of large stepovers, there are no well-defined structural fault segments, but informally the fault trace from Haast to Milford Sound (including Hokuri) is known as the southern section of the Alpine fault. This section has a slip rate of 23 ± 2 mm/yr and has an almost pure dextral sense of movement on a near-vertical fault plane (Berryman et al., 1992; Norris and Cooper, 2001; Sutherland et al., 2006; Sutherland and Norris, 1995). North of Haast, the slip rate is slightly higher (27 ± 5 mm/yr), there is a minor dip-slip component, and the fault dips to the southeast (Norris and Cooper, 2001, 2007). The offshore fault section, south of Milford Sound, also has a higher slip rate at 27–31 mm/yr (Barnes, 2009).

Trench exposures along the Alpine fault have been used to obtain a record of three surface-rupturing earthquakes since A.D. 750 ± 50 (Berryman et al., 2012a; Yetton and Wells, 2010). Records of off-fault evidence of geomorphic responses to earthquakes such as tree-ring dating of landslide scars, episodic progradation of coastal dune ridges, and fluvial terrace formation suggest five earthquakes since A.D. 1230 (Wells and Goff, 2007). It is uncertain whether all these earthquakes were on the Alpine fault, and if they were, the extent of surface rupture associated with each event is also uncertain. The last earthquake thought to have ruptured much of the onshore Alpine fault occurred in A.D. 1717 ± 5 with the penultimate earthquake at approximately A.D. 1230 (Berryman et al., 2012a; Wells and Goff, 2007; Yetton and Wells, 2010).

The Hokuri Creek site (henceforth called Hokuri) is located on the southern part of the onshore Alpine fault (Fig. 1). Hokuri Creek drains the western side of the Skippers Range and flows into Lake McKerrow, a drowned U-shaped glacial valley that is dextrally offset 400 ± 100 m by the Alpine fault (Fig. 1B). The catchment area of Hokuri Creek is 42 km^2, most of the catchment is steep and forested up to elevations of 1100 m, and the highest point in the catchment is 1507 m (Fig. 1C). The area receives 6–7 m of rainfall per year, and the stream flows year-round. Just to the northwest of the confluence of the north and south branches of Hokuri Creek, there is a relict gorge (Fig. 1D). The relict gorge marks the former path of Hokuri Creek when it flowed across the Alpine fault scarp (Sutherland and Norris, 1995). The fault scarp across the floor of the relict gorge is ~1 m high up to the northwest, and Sutherland and Norris (1995) suggested there was an ~8 m and an ~9 m lateral offset on stream channels across the scarp (a cumulative displacement of ~17 m).

In the vicinity of the junction of the north and south branches of Hokuri Creek, and for ~400 m downstream, there are terraces up to 16 m in height above river level. The terraces are underlain by Holocene sedimentary beds of peat and silt (Figs. 2A–2E). Hull and Berryman (1986) and Sutherland and Norris (1995) described the sediments as lake to lake-edge sediments. Radiocarbon ages indicated the sequence ranged from >5000 to <1000 yr B.P., and Sutherland and Norris (1995) inferred that cessation of the silt and peat deposition must have coincided with the abandonment of the former Hokuri Creek gorge. Following abandonment of the gorge, Hokuri Creek incised through the peat and silt sequence; in the past few decades, the sequence has become increasingly better exposed.

RESULTS

Lithofacies of the Hokuri Sediment Sequence

Distinctive cyclic stratigraphy characterizes most outcrops at Hokuri, which, at a broad scale, appear to be couplets of silt and peat. In detail, this cyclic stratigraphy consists of alternating 0.3–1-m-thick beds of dark-brown to brown-gray, organic-enriched silt and peat, and pale-gray to gray-brown silt (Figs. 2 and 3). Within each decimeter-scale bed type, there are commonly millimeter-scale organic or nonorganic laminae. In this section, we outline the sedimentary properties used to define the lithofacies, and then describe the lithofacies (and sublithofacies) present in the Hokuri sequence.

Defining the Lithofacies

Ten riverbank outcrops of the Hokuri sedimentary sequence were described, measured, and sampled (see Data Repository item 1 for methods[1]). No single outcrop exposed the complete sequence. The longest continuous outcrop is E_1, which is 13 m in height. In addition, we obtained sediment from two auger holes that penetrated to 5 m below the river level, totaling a composite stratigraphic sequence of 18 m.

The Hokuri sedimentary sequence was divided into decimeter-scale beds in the field, and each bed was visually described following a modified Troels-Smith classification system (Aaby and Berglund, 1986; Troels-Smith, 1955). Visual, qualitative field descriptions of the color, darkness, stratification, humification, and dominant and subordinate sediment types of all beds were obtained. The visual descriptions were complemented with quantitative laboratory-based measurements of sediment properties using X-ray scanning, high-resolution photography (to obtain grayscale values) and magnetic susceptibility on cores of selected outcrops (Fig. 4).

X-ray, grayscale, and magnetic susceptibility measurements were used as proxies for the amount of organic matter in the sediments (see Data Repository item 1 for methods [see footnote 1]). X-ray attenuation is a proxy for sediment density; in higher-density sediment, the low-energy X-rays are highly attenuated and vice versa. Density variations of the Hokuri sediments are probably due to changes in organic sediment content. A higher proportion of plant material lowers the sediment density; conversely, more clastic sediment and less organic material increase the density. Grayscale measures the darkness of the sediment; organic sediment content is the most likely cause of darkness changes. Magnetic susceptibility (measured in κ units) varies in relation to the concentration and composition of the magnetic (commonly iron-bearing) minerals. In situations where the mineralogy is uniform, κ is a proxy for concentration of magnetic minerals. Magnetic grains extracted and examined by electron microprobe analysis returned bulk compositions very close to ilmenite. The uniformity in magnetic composition between the different lithofacies of the Hokuri sequence supports a common source of magnetic mineral (ilmenite). The variations in magnetic susceptibility correlate strongly with those in X-ray attenuation and reflect variations in the relative proportions of clastic and organic sediment.

Twenty-one samples analyzed for total carbon content confirm a relationship between the three proxy measurements described here and the organic material content of the sediment. The samples, from across the range of lithofacies (except gravel samples), showed that high % total carbon correlated to high grayscale (increased darkness), and low X-ray attenuation and magnetic susceptibility (Fig. 5). This

[1]GSA Data Repository item 2013133, summary of methods, cluster analysis tree, diatom species list with habitat and moisture preferences, and full details of radiocarbon ages, is available at http://www.geosociety.org/pubs/ft2013.htm or by request to editing@geosociety.org.

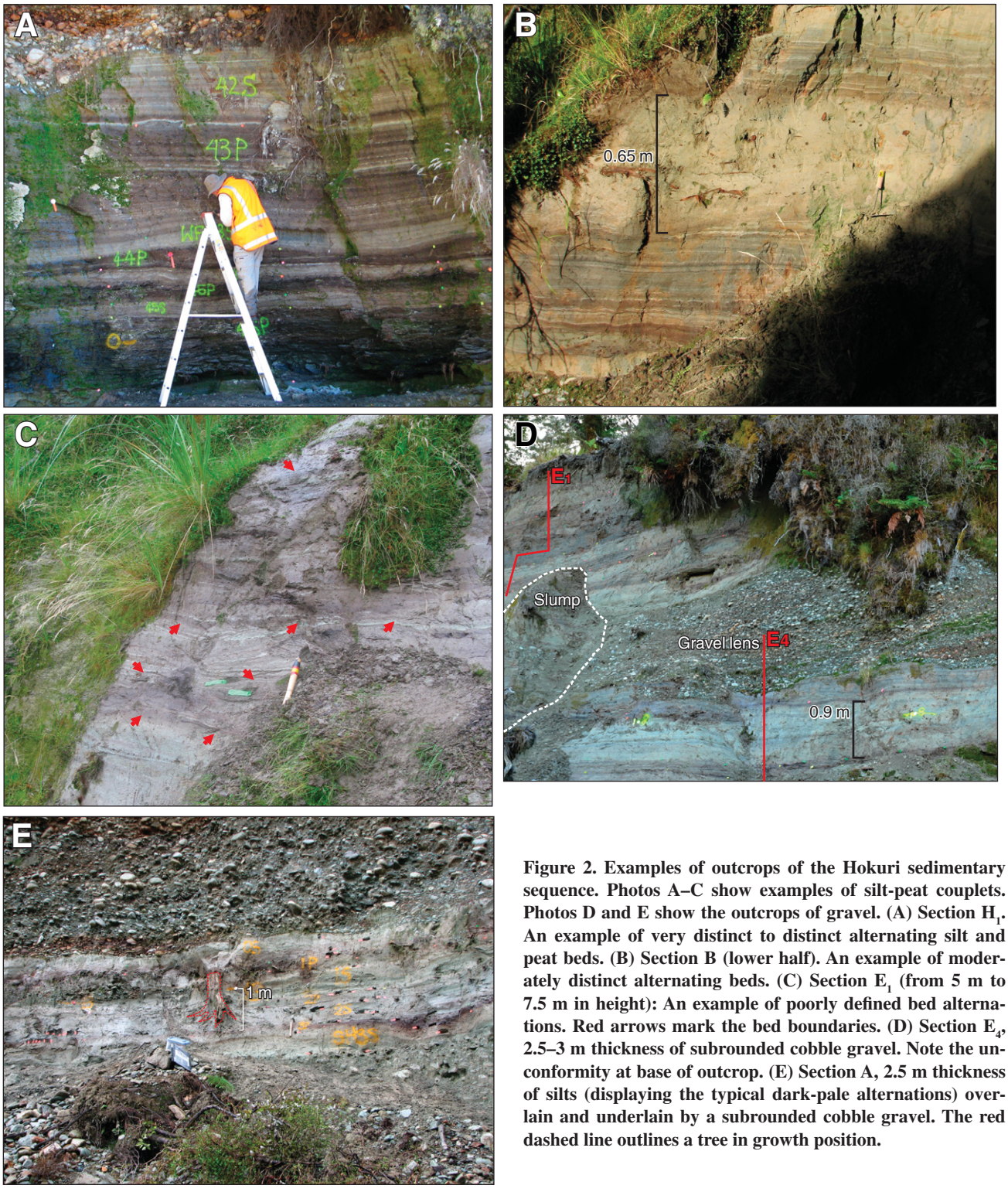

Figure 2. Examples of outcrops of the Hokuri sedimentary sequence. Photos A–C show examples of silt-peat couplets. Photos D and E show the outcrops of gravel. (A) Section H_1. An example of very distinct to distinct alternating silt and peat beds. (B) Section B (lower half). An example of moderately distinct alternating beds. (C) Section E_1 (from 5 m to 7.5 m in height): An example of poorly defined bed alternations. Red arrows mark the bed boundaries. (D) Section E_4, 2.5–3 m thickness of subrounded cobble gravel. Note the unconformity at base of outcrop. (E) Section A, 2.5 m thickness of silts (displaying the typical dark-pale alternations) overlain and underlain by a subrounded cobble gravel. The red dashed line outlines a tree in growth position.

Figure 3. Summary of the stratigraphy of the Hokuri Creek outcrops. The dominant sediment composition of each bed is denoted by letters and numbers next to the bed using, e.g., Ag3Dg1: 75% silt, 25% wood and plate detritus. Bed correlations that were followed continuously between outcrops are shown by black dashed lines. Note vertical scale is accurate, but horizontal distances between outcrops are not to scale.

Geological Society of America Bulletin, published online on 22 February 2013 as doi:10.1130/B30693.1

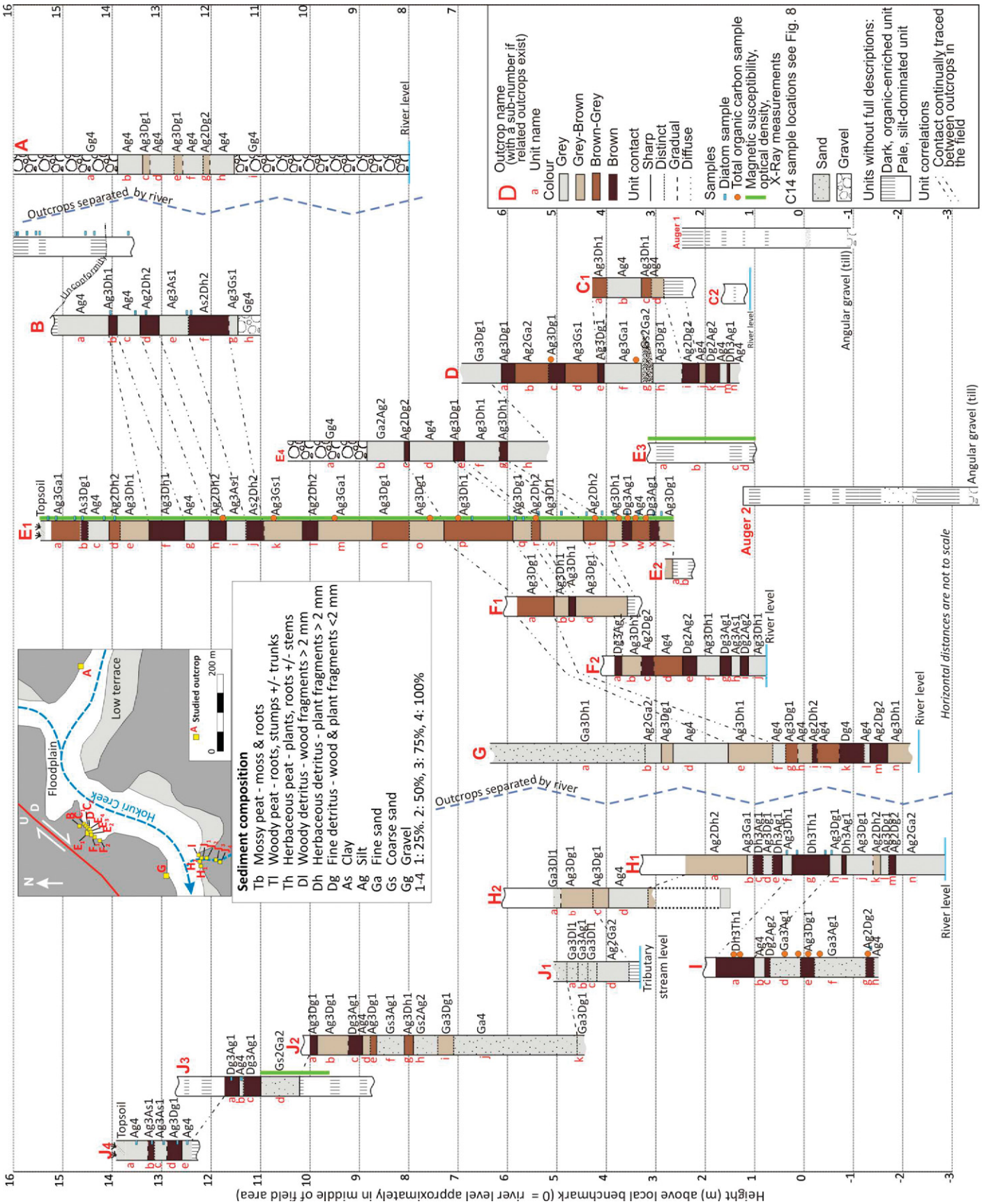

Geological Society of America Bulletin, published online on 22 February 2013 as doi:10.1130/B30693.1

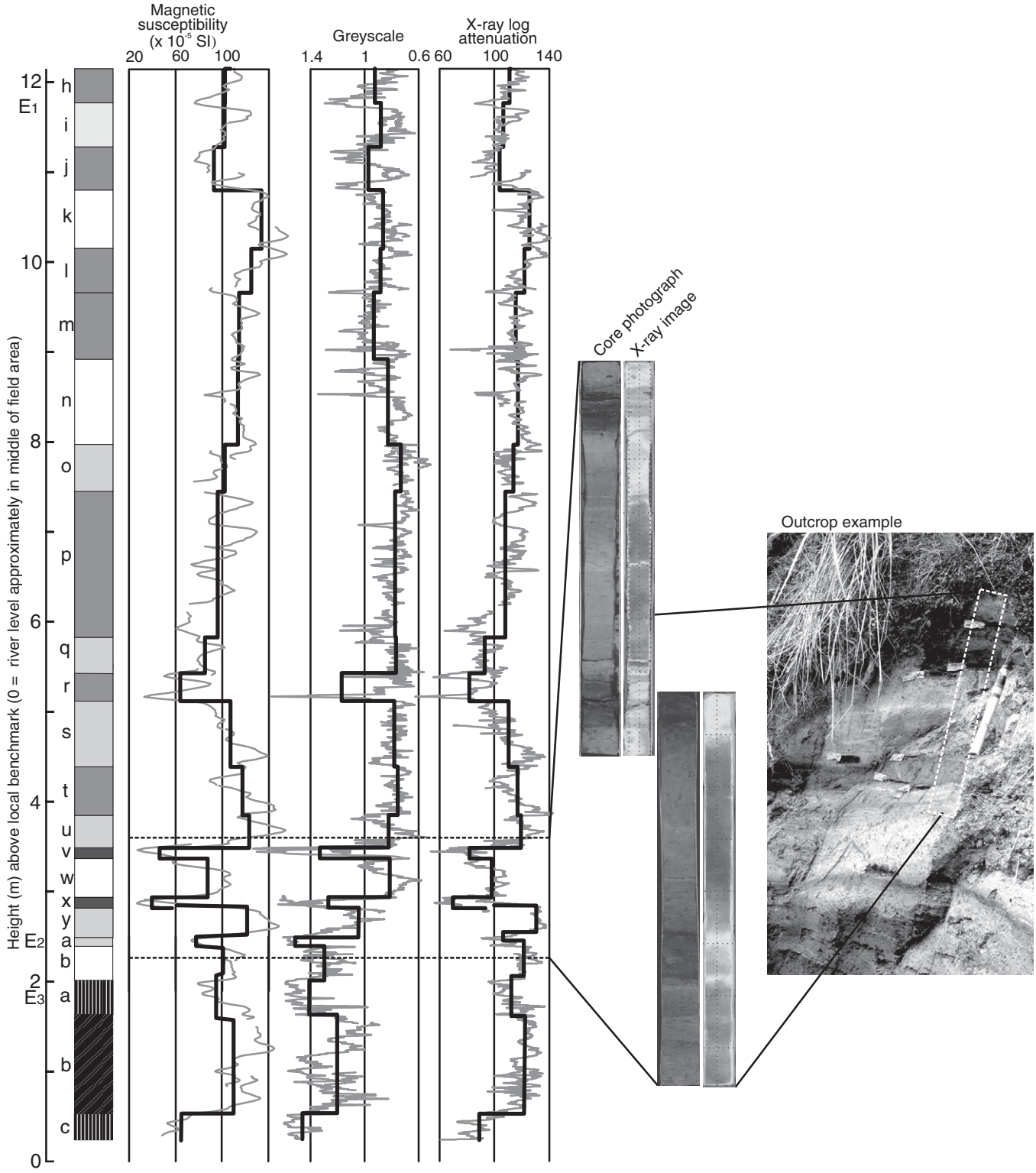

Figure 4. Measurements of magnetic susceptibility, grayscale and X-ray log attenuation from sections E_1, E_2, and E_3. The outcrops have been spliced together using correlations of prominent and continuous sediment beds and laminae to form a composite section. The variability measured at high-resolution by the grayscale photography and X-ray scanning shows the different scales at which one can examine the Hokuri stratigraphy: There are ubiquitous millimeter- to centimeter-scale layers in the sediment, but this study focuses on the larger scale, decimeter- to meter-scale changes. The solid black line represents the average value for each bed (bed contacts defined in the field). The elevations of the bed contacts vary slightly from that shown in Figures 3 and 8 because the cores were not taken at exactly the same location as initial sequence descriptions and sampling. For comparison, a core photo, the X-ray image, and the sampled outcrop are shown at right. The key to stratigraphy is shown in Figure 8.

Geological Society of America Bulletin, published online on 22 February 2013 as doi:10.1130/B30693.1

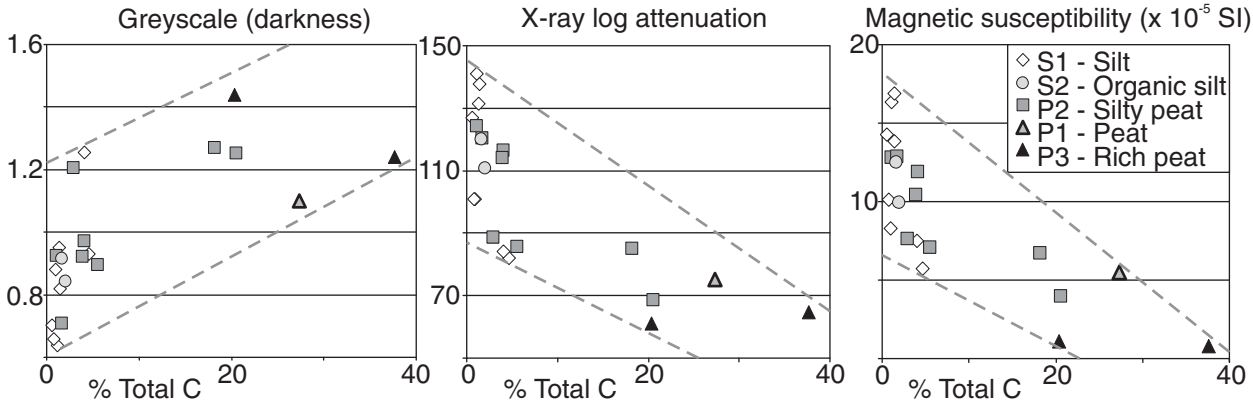

Figure 5. Relationships between the physical properties of the sediment and the measured amount of total carbon (% total C). Grayscale correlates positively with % total C, and X-ray log attenuation and magnetic susceptibility have a negative relationship to % total C. Sample locations are shown on Figure 3.

confirms our correlations between the physical properties of the sediment and the varying proportions of organic matter. Total carbon is composed of inorganic and organic carbon. Inorganic carbon in sediment could be derived from weathering of carbonate rocks; however, because there are no carbonate rocks within the catchment, rock-derived carbon probably contributes only a minor amount of the total carbon. The dominant contribution to total carbon is organic carbon derived from plant remains.

Lithofacies Descriptions

At the highest order, there are three major lithofacies in the Hokuri sequence: silt-dominated beds (S), peat-dominated beds (P), and gravel beds (G). Cluster analysis shows the high-order division of lithofacies, and at a lower order, six sublithofacies are readily apparent (Data Repository item 2 [see footnote 1]). The typical properties of each lithofacies and sublithofacies are described next and shown in Figure 3.

Lithofacies S. Silt-dominated beds can be divided into silt (S1) and organic silt (S2). Silt-dominated lithofacies have comparatively low grayscale and high X-ray log attenuation and magnetic susceptibility values compared to the peat-dominated lithofacies.

Sublithofacies S1 (silt, n = 49). The silt beds are dominantly gray (subordinate color is gray-brown) and pale. The dominant sediment size is silt, but there are some fine and coarse sands. Only rarely is organic detritus a significant component of the sediment, and it is typically slightly decayed. This category contains varying degrees of stratification, with most beds being partially/indistinctly laminated, although there are several beds that are homogeneous.

Sublithofacies S2 (organic silt, n = 35). Organic silt beds are typically pale-gray-brown or gray. They are dominated by silt, but most have a small proportion of organic detrital material that is slightly decayed (wood and plant fragments <2 mm). Most beds are laminated.

Lithofacies P. Peat-dominated beds can be divided into peat (P1), silty peat (P2), and rich peat (P3). Peat-dominated beds have comparatively high grayscale and low X-ray log attenuation and magnetic susceptibility values.

Sublithofacies P1 (peat, n = 14). The peat beds are all dark to very dark brown. The dominant sediment component is decayed organic detrital material, with subordinate components of silt. The peat beds display varying degrees of stratification, from homogeneous to distinct laminations.

Sublithofacies P2 (silty peat, n = 39). The silty peat beds are quite similar to the organic silt beds, but the main difference is the color and darkness (nigror). Silty peats are typically medium to dark brown, or gray-brown. The dominant component is silt, with subordinate fractions of slightly decayed organic detrital material. Most beds are laminated.

Sublithofacies P3 (rich peat, n = 2). The rich peat beds are very dark brown to black. They are entirely composed of decayed organic material, mostly plant detritus such as stems, reeds, and leaves. These beds are homogeneous to indistinctly laminated.

Lithofacies G (gravel, n = 4). The gravel beds are medium-gray, clast-supported, subrounded to subangular pebble to cobble gravel. The matrix is typically coarse sand. There is some crude bedding.

Paleoenvironment Based on Diatom Assemblages

Samples for diatom analysis were selected from a variety of sublithofacies to maximize understanding of the range of paleoenvironments represented in the sedimentary sequence. We used habitat types and moisture preferences of diatom species to reconstruct the past environment of each sediment sample (Table 1; Data Repository item 3 [see footnote 1]).

Species assemblages of diatoms indicate that the depositional environment of the Hokuri sedimentary sequence was a very shallow, predominantly low-energy, aquatic system throughout its history. We infer that the ~20 ha study site was isolated from the main floodplain of Hokuri Creek and consisted of a series of ponds, pond margins, wetlands, and moist meadows. The evidence for this interpretation comes from two main sources. The first is that diatoms are abundant and well preserved in most of the samples investigated. These generally high diatom concentrations indicate that the Hokuri Creek sediments represent a paleoenvironment favorable to diatom habitation, i.e., a low-energy aquatic system of some sort. The second is that over 120 species were identified from these samples (Data Repository item 3 [see footnote 1]), and most are from benthic or tychoplanktic habitats (Fig. 6; Table 1 for definition of habitat terms), indicating that the past environment must have been shallow most of the time because these diatoms require light penetration to the floor of the water body.

The dominance of tychoplankton and benthos throughout the sequence is a notable feature of the Hokuri Creek sediments (Fig. 6). There is no shallowing-upward sequence (e.g., with

Geological Society of America Bulletin, published online on 22 February 2013 as doi:10.1130/B30693.1

TABLE 1. DIATOM-INFERRED WATER-BODY TYPES PRESENT IN THE HOKURI CREEK STRATIGRAPHIC SEQUENCE (FAR-RIGHT COLUMN) INFERRED FROM THE COMBINED HABITAT AND MOISTURE PREFERENCES OF DIATOM SPECIES (MID-RIGHT COLUMN)

Habitat type	Moisture preference (Van Dam et al., 1994)	Combined habitat-moisture categories used in this study	Inferred water-body type (arranged in order of decreasing water depth)
Plankton *(live in water column)*	Never outside water bodies	Plankton never outside water bodies	Lake
Meroplankton (*part of life cycle in water column)*	Mainly in water bodies	Meroplankton mainly in water bodies	Pond
Benthos *(live on floor of water body)*	Mainly on wet and moist places	Benthos in water bodies	Shallow pond
Tychoplankton *(thrive in shallow and/or turbulent habitats)*	In water bodies and wet places	Tychoplankton	Pond margin
Benthos	Always outside water bodies	Benthos in wet and dry places	Swamp/soil
Unknown	Unknown	Unknown	Unknown

Note: Our combined categories were derived from known habitats (far-left column) and the moisture preference scale (mid-left column). Full listing of species' preferences is presented in Data Repository item 3 (see text footnote 1).

transitions from lake to pond to wetland to soil environments), as might be expected in an infilling water body that results in a sedimentary thickness of ~18 m. Instead, it seems that relatively continuous accretion occurred in very shallow water throughout the period of sediment deposition. Isolated occurrences of plankton could imply that deeper ponded water existed for short periods (Fig. 6). However, the main planktonic species, *Discostella stelligera*, can also live in streams and so may have been transported to the site (Sonneman et al., 2000). There are also a few samples dominated by meroplankton (Fig. 6), which could be considered to represent deeper water. However, several of the species in this category (e.g., *Aulacoseira alpigena and Aulacoseira distans*) appear to prefer shallow-water environments, with occurrences

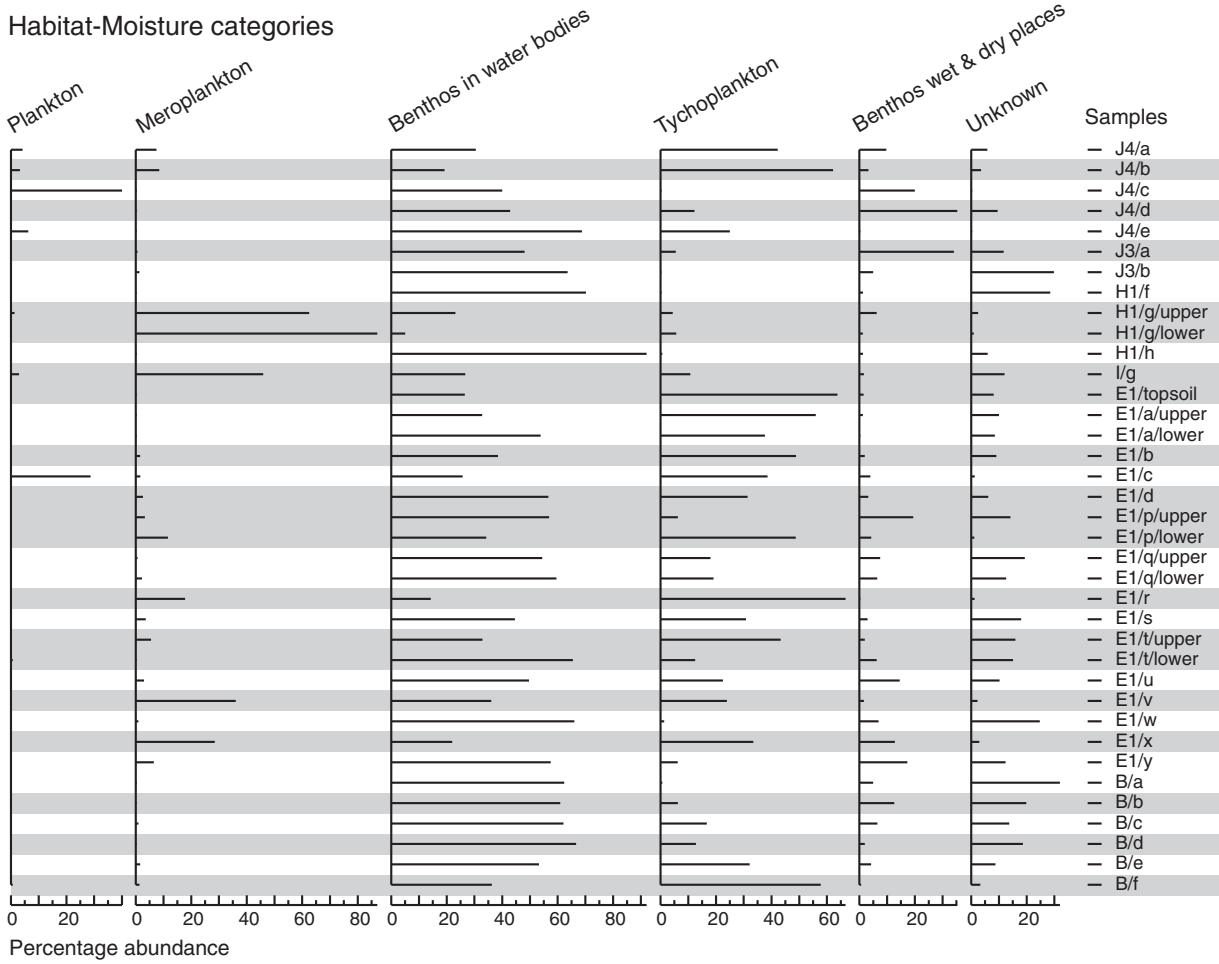

Figure 6. Percentage abundance of diatom valves in habitat-moisture categories (see Table 1 and Data Repository Item 3) for representative samples throughout the study area (listed according to section/bed as shown in Fig. 3). Samples are plotted in stratigraphic order within each section but not between sections. The gray shaded rows represent samples from peat beds and rows without shading represent silt samples.

Geological Society of America Bulletin, published online on 22 February 2013 as doi:10.1130/B30693.1

reported from shallow lakes, large ponds, and even floating wet mosses (Brugam et al., 1998; Moos et al., 2005; Van De Vijver et al., 2002). Therefore, these samples probably represent deeper water than samples consisting entirely of benthos and tychoplankton, but probably only in the order of 2–8 m water depth.

Diatom assemblages differ between the silt and peat lithofacies at Hokuri Creek, indicating that changes in lithofacies also represent changes in depositional environment. Although all samples are consistent with a shallow-water environment, as described already, the silt beds are always dominated by benthos in water bodies, whereas the peat beds generally have higher proportions of tychoplankton (Fig. 7). This differentiation suggests that the silt beds were deposited in slightly deeper water than the peat beds—within shallow ponds instead of at pond margins (Table 1). Therefore, we infer that a hydrological change occurred at each contact in addition to the obvious change in sediment source that is indicated by the sedimentology.

Depositional Model for the Silt-Peat Couplets

We used the distribution of lithofacies combined with paleoenvironmental data supplied by the diatom assemblages to develop a depositional model for the Hokuri sediment sequence. The dominant feature of the sediments is alternations between pale, silt-dominated beds (S1 and S2) and darker, organic-rich beds (P1, P2, P3), which characterize all outcrops at Hokuri (Fig. 3). We summarize the silt-dominated beds as "silts" and the peat-dominated beds as "peats," recognizing that these terms encompass some variability. Each pair of beds is referred to as a silt-peat couplet. A combination of the sedimentological and diatom data confirms that in sections E–J (Fig. 3), the paleoenvironment was an aquatic, shallow, low-energy basin that sustained repeated cycles between two main modes of deposition. The first mode of deposition, represented by the silt beds, involved deposition of clastic material in shallow ponds. The second mode of deposition, represented by the peat beds, involved in situ accumulation of organic material in very shallow ponds, pond margins, and wetlands. The silt-peat couplets thereby represent a cycle of hydrological and depositional change, with the arrival of silt involving an influx of sediment and water to a site that was otherwise isolated from moving water and catchment-derived sediment. Twenty-two major silt-peat couplets were identified in the Hokuri sequence, and given that the arrival of silt at the site marks a depositional "event," the peat-to-silt contacts are referred to as "event horizons." We label these event horizons Hk1–Hk22 (Fig. 8).

Radiocarbon Ages of the Hokuri Creek Sequence and Implications for Section Correlations and Paleotopography

Radiocarbon ages were used to assist with correlating the silt-peat couplets between outcrops, to estimate the age of event horizons Hk1–Hk22, and to identify changes in basin paleotopography through history. One hundred and twenty-three samples of organic material were radiocarbon dated. The most commonly dated organic materials were leaves, reeds, and seeds; only eight wood samples were dated. All radiocarbon ages were calibrated using the Southern Hemisphere calibration curve of (McCormac et al., 2004) in the OxCal v. 4.1 program (Bronk Ramsey, 2009). All age ranges in this paper are presented as 2σ (95.4%) distributions in calibrated years B.C. or A.D.

The deepest part of the section dates back to ca. 8500 B.C. in auger 2, and the youngest sediments at the top of section E_1 are ca. A.D. 800; thus, the alternating silt-peat sequence spans 9300 yr (Fig. 8; full details of all radiocarbon ages are in Data Repository item 4 [see footnote 1]). Detailed stratigraphic analysis was only carried out for the well-exposed section spanning ~7000 yr. The majority of ages are in stratigraphic order, with very few apparent age reversals. Where age reversals were present, we usually dated a duplicate sample from the same location but used a different organic fraction, which yielded an age consistent with samples above and below.

The correlation of beds between outcrops was usually undertaken by tracing continuous and distinctive stratigraphic beds or laminae between the outcrops (Fig. 3). Correlation of beds above and below the distinctive beds could be achieved by counting the number of silt-peat couplets. Similarities in the sediment characteristics helped confirm the correlations. Sections on the same riverbank could all be correlated reliably using continuous contacts. Correlation issues only arose when outcrops were on different sides of the river (i.e., between sections G and H_1, and sections A and B), and in these situations, radiocarbon data were required.

Bed correlations across the river between sections E_1 and J_2-J_4 and between sections G and H_1 were clear when radiocarbon data were used. Good matches between radiocarbon ages bounding the contacts between E_1n–E_1m and J_2c–J_2b enabled a correlation line to be established. The silt-peat couplets above that correlation line are consistent in number and age. Stratigraphy was the main characteristic used to correlate between sections G and H_2. The sand-dominated nature of beds Ga and Gb and H_2a and H_2b was strikingly similar, as was the thick, rich peat character of Gk and H_1g. The ages of the beds in between were largely consistent with the correlations made at the top and base, but there were inconsistencies in the correlations, which imply some beds are not continuous as a distinct layer across the whole basin.

The silt-peat couplets of section A could not be precisely correlated to any other couplets in the Hokuri basin. Two radiocarbon ages from bed Ag suggest an approximate correlation to beds E_1o–E_1r, but too few ages were obtained from section A to make a more confident correlation. The two ages from bed Ag are also ~800 yr apart, despite being at the base and top of a single peat bed. This age spread is much greater than any other peat bed, which suggests one of the two ages is anomalous, or that silt beds existing in other sections are missing in section A.

Radiocarbon samples were collected from near the top of the peat beds and the base of the silt beds in order to determine the timing of silt arrival. The OxCal program (Bronk Ramsey, 2001) was used to model the age of each peat-to-silt contact by analyzing the probability distributions of the radiocarbon ages bounding the peat-to-silt contact (Data Repository item 1 [see footnote 1]). The ages of the 22 peat-silt contacts are presented in Figure 8. The peat-to-silt contacts occur at intervals of 150–660 yr, with an average interval between contacts of ~330 yr.

Most silt-peat couplets show remarkable continuity and can be correlated around the basin, but there are two couplets that become less distinct laterally (couplets associated with event horizons Hk8 and Hk15) and one event horizon that is poorly expressed in all outcrops (Hk10).

Hk8

The Hk8 event horizon is present in sections J, H_2, and G but is not present in section E_1 (Fig. 8). Hk8 correlates into section E_1 at the time interval represented by beds E_1o and E_1n; this interval is particularly silt dominated. We surmise that the part of the basin where E_1n–o accumulated was more of a floodplain than a wetland; hence, it was not a sensitive recorder of the change in water depth that led to the development of the Hk8 horizon elsewhere in the basin.

Hk15

The Hk15 event horizon is present in section F_2 but cannot be correlated to any other nearby outcrops (Fig. 8). Hk15 is at the top of a relatively thin (~0.4 m thick) silt-peat couplet, but it is very distinctive, with a strong contrast between the peat and the silt. The radiocarbon ages bounding Hk15 in section F_2 imply it must

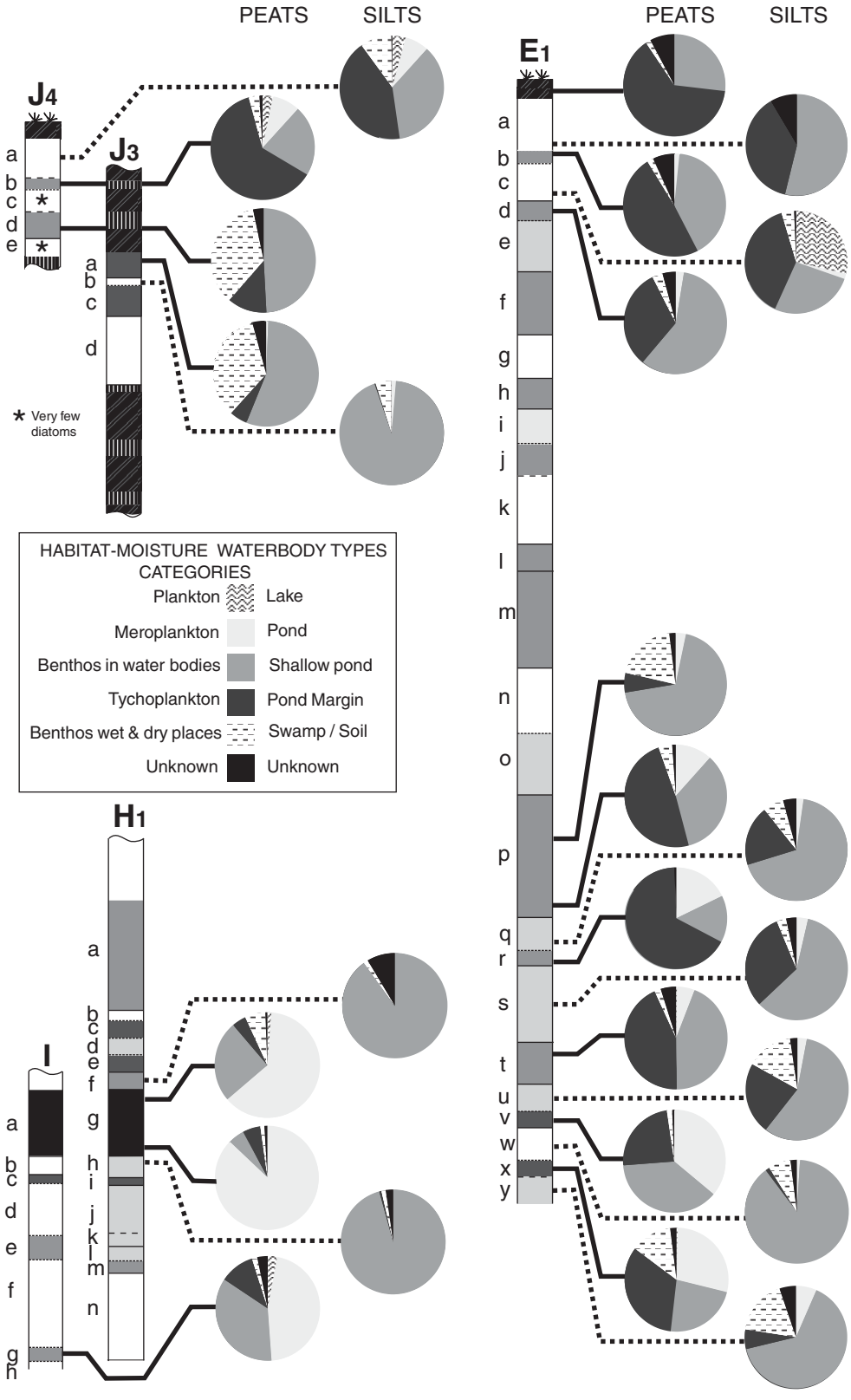

Figure 7. Diatom assemblages plotted as pie graphs for representative samples from different sections to illustrate the difference between peat beds and silt beds. Assemblages from silt beds are dominated by "benthos in water bodies," indicative of shallow ponds, whereas assemblages from peat beds have higher proportions of tychoplankton and "benthos in wet and dry places," implying pond margin, swamp, and soil environments of deposition.

Figure 8. Beds of the Hokuri sequence clustered into sediment types. All radiocarbon ages are shown along with the correlations of the peat-to-silt contacts (continuous or inferred). Details of all radiocarbon samples are listed in Data Repository item 4 (see text footnote 1). Event horizons are shown as red lines. Ages of event horizons listed in green are modeled ages derived from bounding radiocarbon samples (Berryman et al., 2012b).

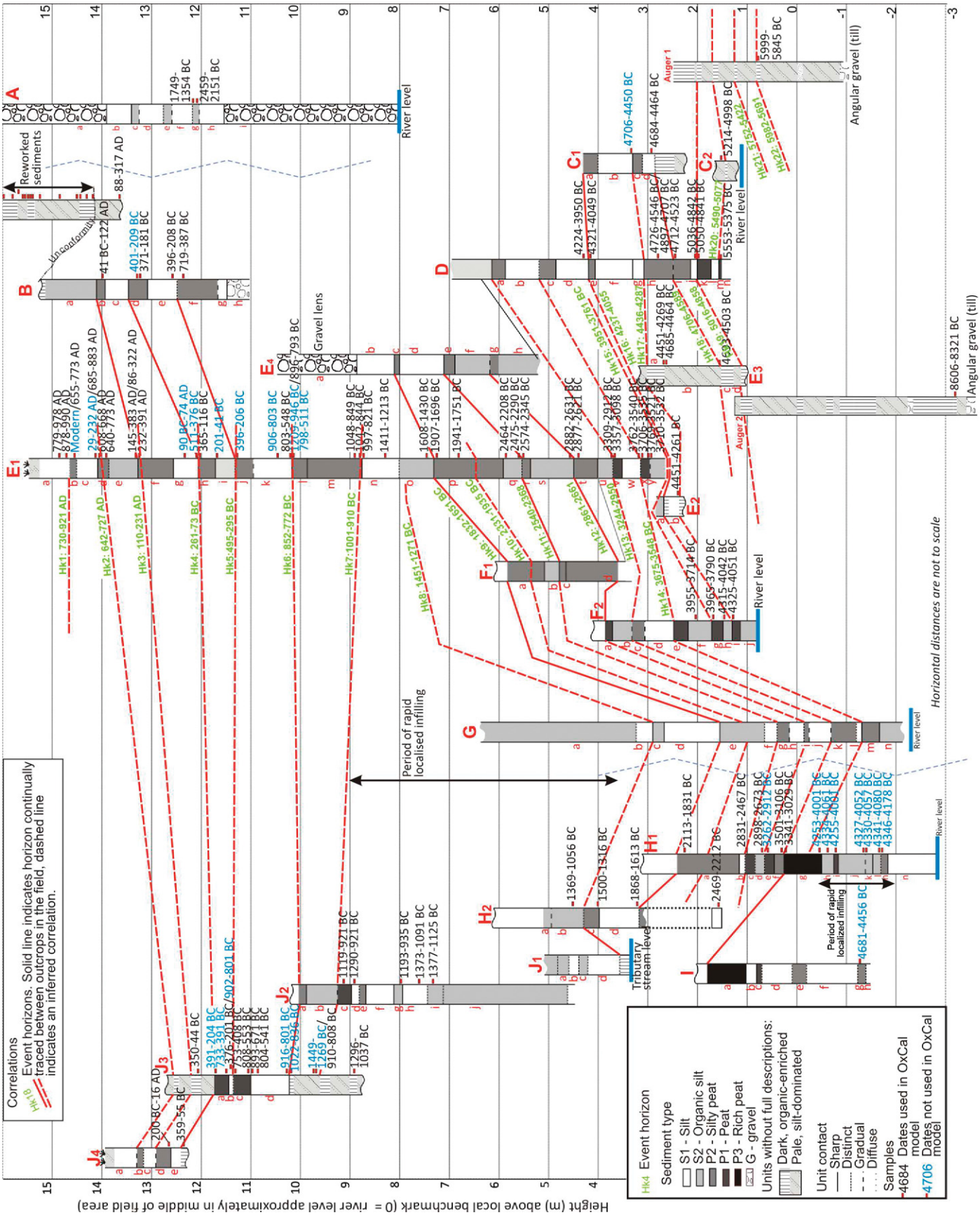
Correlations
Event horizons. Solid line indicates horizon continually traced between outcrops in the field, dashed line indicates an inferred correlation.
Hk18
Reworked sediments
Unconformity
River level
Gravel lens
Angular gravel (till)
Auger 1
Auger 2
Period of rapid localised infilling
Tributary stream level
Horizontal distances are not to scale
Height (m) above local benchmark (0 = river level approximately in middle of field area)
Event horizon
Sediment type
S1 - Silt
S2 - Organic silt
P2 - Silty peat
P1 - Peat
P3 - Rich peat
G - gravel
Units without full descriptions:
Dark, organic-enriched
Pale, silt-dominated
Unit contact
Sharp
Distinct
Gradual
Diffuse
Samples
4684 Dates used in OxCal model
4706 Dates not used in OxCal model

be below the base of E_1 and above the De-Dd contact in section D. However, continually traceable contacts among sections E_1, E_4, and D mean that Hk15 cannot correlate to the Dc-Db contact, so it must have pinched out in between sections F_2 and D.

Hk10

The event horizon Hk10 has been inserted into the middle of bed E_1p and H_1a because there is tentative evidence of a paleoenvironmental change within this anomalously thick peat bed. The characteristic feature of the peat bed below Hk9 is that it is thick (~1 m) and silt dominated in all outcrops (see comparison of sections E_1 and H_1; Fig. 9). This contrasts with most peat layers, which are <0.5 m thick and have higher proportions of organic matter in at least some outcrops (i.e., they can be silt dominated in places but elsewhere have higher organic content). There is some paleoenvironmental evidence for an event during deposition of the silt-peat couplet between event horizons Hk11 and Hk9: A 0.1–0.2-m-thick pale silt bed in the middle of bed E_1p (Fig. 9) bears a diatom assemblage that has a closer resemblance to the underlying silt layer than the encasing peat bed (Fig. 7, compare three samples in beds E_1q and E_1p). In the equivalent bed in section H_1, there is a thin (~4 cm), but very prominent pale silt bed that could mark the missing event (Fig. 9). Around the time period in question for Hk10 (ca. 2000 B.C.), the sections in the main part of the Hokuri basin (E, F, G, and H) appear to have been somewhat insensitive to paleoenvironmental change, while at the same time in section A, there are three distinct silt-peat couplets. This suggests that the floodplain-wetland paleogeography may have been slightly different around ca. 2000 B.C., and perhaps the more sensitive part of the wetland was located upstream around section A, while the main part of the basin received a higher portion of silt. We have included Hk10 as an event horizon but acknowledge that it is not supported by the stratigraphy in all sections.

Changes over time in the paleotopography of the Hokuri depositional basin become apparent when the age of the sediments is known. In particular, a significant change must have occurred between ca. 1500 B.C. and 1000 B.C. because sediments older than ca. 1500 B.C. in sections G, H, I, and J are ~3 m lower than equivalent-aged sediments in sections C–F (the two groups of sections are 230–320 m apart). Sediments younger than ca. 1000 B.C. in sections G, H, I, and J are at the same elevation as their equivalents in sections B and E (Fig. 8). Spanning this time period, sections G, H, and J have ~5–6 m of sediment, while section E_1 has only 1.5 m of sediment. The absence of large time gaps in the radiocarbon ages of section E_1 suggests that an unconformity is not responsible for the difference in sediment thickness. The 5–6 m sequence encapsulated in sections G, H_2, J_1, and J_2 is unusual in the Hokuri sequence because it is characterized by sandy sediments. Radiocarbon ages indicate the sandy sequence was deposited relatively

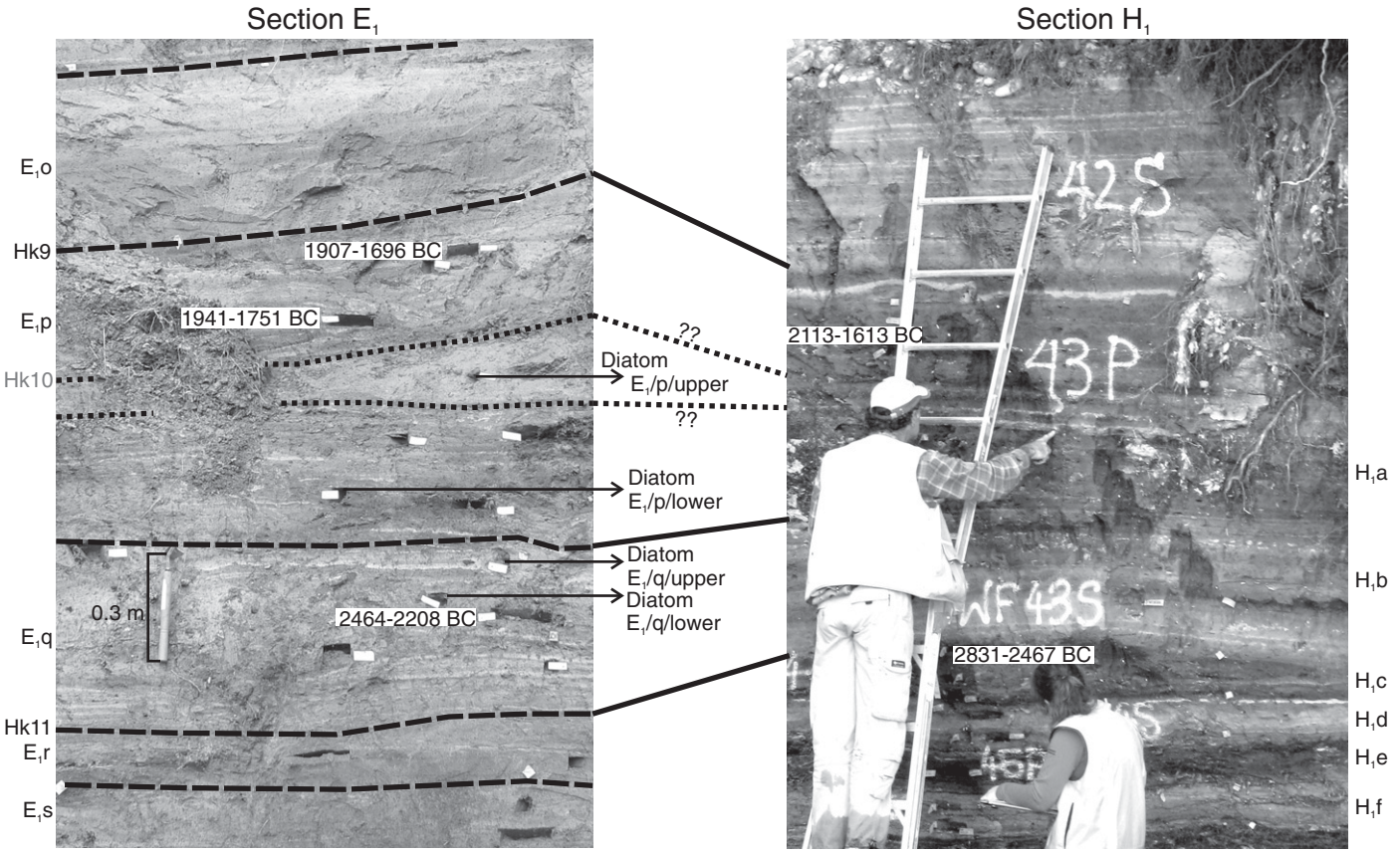

Figure 9. Exposures of the Hk11 and Hk9 contacts at sections E_1 and H_1. In section E_1, there is very little contrast between the peat and the silt beds, but within the E_1p bed, there is a faint silt package that could represent a missing event labeled Hk10. This is supported by diatom analyses, which show that the silt within E_1p has a greater similarity to the E_1q bed than it does to surrounding E_1p samples. In section H_1, the peat and silt packages are more distinct, but with bed H_1a, it is possible to distinguish a pale silt bed that may be the equivalent of Hk10 (the person on the ladder is pointing to the approximate location of the Hk10 contact).

Geological Society of America Bulletin, published online on 22 February 2013 as doi:10.1130/B30693.1

rapidly, but not instantaneously, i.e., it is not a debris-flow deposit.

Our preferred explanation for the differential thickness of sediment deposited from 1500 to 1000 B.C. between the outcrops of G–J and C–F is that a natural low point created by peat compaction around outcrops G–J existed prior to 1500 B.C., a sediment pulse at 1500 B.C. infilled the low point, and from 1000 B.C. to A.D. 800, the wetland aggraded at the same elevation. At the base of sections G, H, and I, there are particularly thick and organic-rich peat beds, and these are thicker and more organic-rich than the peats beneath sections C–F. Peats have high compaction ratios, and studies of deltaic environments (analogous to the Hokuri sequence in having interfingering peat and silt beds) have shown that peat compaction can have a significant impact on geomorphology, because deltaic channels respond to uneven ground subsidence (Allen, 1999; Long et al., 2006; Törnqvist et al., 2008; van Asselen et al., 2009). Post–1000 B.C., sediment compaction no longer played a role in creating a low point in the wetland because it had infilled with sand.

The basic depositional model for the Hokuri sequence is one of repeated silt-peat couplets that represent cycles of hydrological and depositional change. Twenty-two event horizons located at the peat-to-silt contact in between couplets mark the influx of sediment into a wetland previously dominated by in situ organic-dominated sedimentation. Radiocarbon ages and stratigraphic continuity show that peat-silt couplets correlate throughout the basin, and this indicates that the process controlling the depositional cycles operated basinwide. Given the number of silt-peat couplets, there is remarkable lateral continuity in the couplets and their associated event horizons around the Hokuri depocenter. Only two couplets pinch out laterally (couplets associated with Hk8 and Hk15), and one couplet (associated with Hk10) is poorly expressed stratigraphically due to an inferred unfavorable or insensitive depositional environment. The radiocarbon ages also highlight where paleotopographic changes occurred in the basin. The creation and subsequent infilling of a low-lying area in the south of the basin between 1500 and 1000 B.C. are apparent but did not greatly affect the characteristic sequence of silt-peat couplets.

Tectonic Geomorphology of the Hokuri Creek Area

The silt-peat couplets accumulated within meters to hundreds of meters of the Alpine fault scarp, and at least the upper several silt-peat couplets are fault bounded along their western margin (Figs. 1C and 1D). The beds cannot be traced across the main fault scarp, but their relations to the fault are exposed in a gully wall cross section (for location, see Fig. 1D; Fig. 10). The gully wall section shows that silt-peat couplets are increasingly deformed and silt beds merge into colluvial beds closer to the fault scarp. Interfingered with the colluvial beds, there are peat, silt, and organic silt beds. Close to the fault, the sequence begins to look like many paleoseismic trenches in which the accumulation of organic material is disrupted by the arrival of coarse-grained scarp-derived colluviums; thus, the contact between the peat and the colluvium marks the ground surface at the time of the earthquake (e.g., Langridge et al., 2011). At the southeastern end of the exposure, further away from the fault, silt and peat beds are identical in appearance to the silt and peat beds of the nearby riverbank outcrops (B–F) and so are inferred to be the same beds. One dated peat sample from the gully-wall exposure has an age of A.D. 779–961 (Fig. 10), consistent with the upper beds of section E. At the base of the gully wall section, there are stiff, pale-gray, laminated silts inferred to represent a glacial lake environment. An optically stimulated luminescence age obtained from these sediments yielded an age of 100.5 ± 6.4 ka.

Evidence for the sense and amount of displacement along the Alpine fault in a single, surface-rupturing earthquake at Hokuri is provided by a microtopographic survey of offset of stream channels and terrace risers in the abandoned gorge (Fig. 11). The edges of the former main channel (the lowest part of the gorge) are offset dextrally by 7.2–7.5 m. On a higher surface (a former floodplain?), three shallow channels (0.4–1 m deep) are also offset by ~7.5 m (Fig. 11). The riser at the northeastern edge of

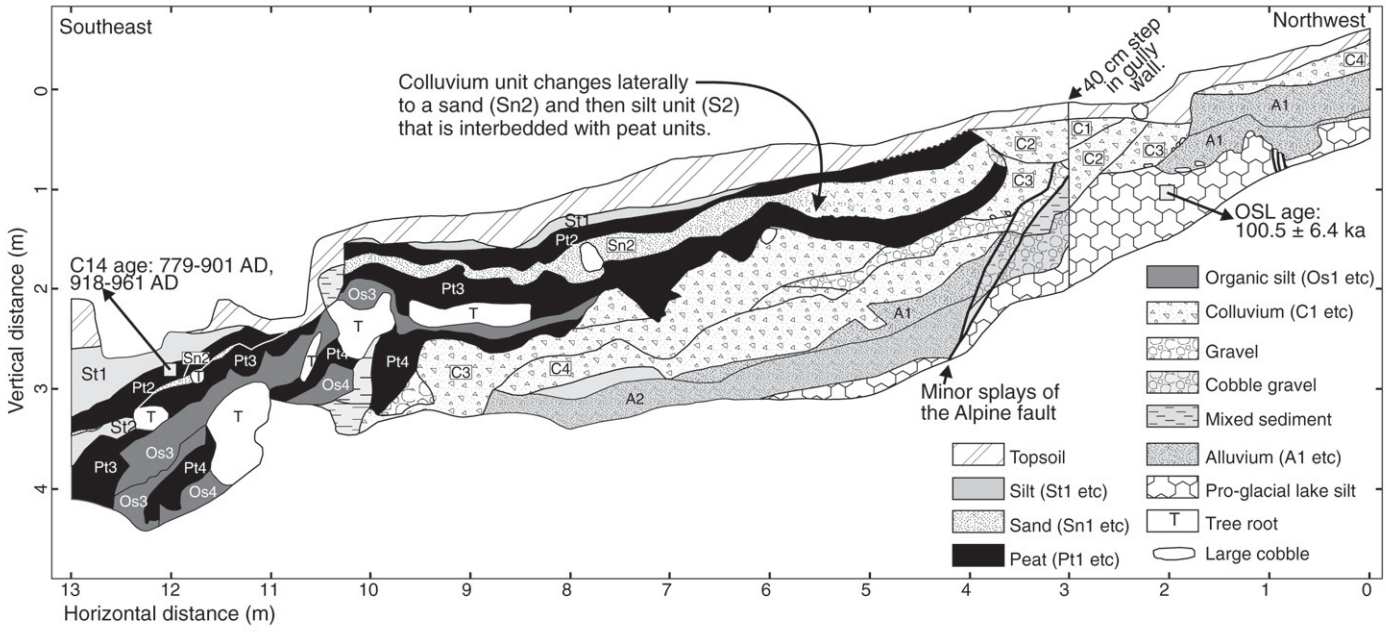

Figure 10. Exposure of the Hokuri silt-peat couplets as they approach the Alpine fault. The exposure shows that as the silt-peat couplets get closer to the fault, they become increasingly deformed and interfinger with colluvial wedges being shed from the fault scarp. OSL—optically stimulated luminescence.

Geological Society of America Bulletin, published online on 22 February 2013 as doi:10.1130/B30693.1

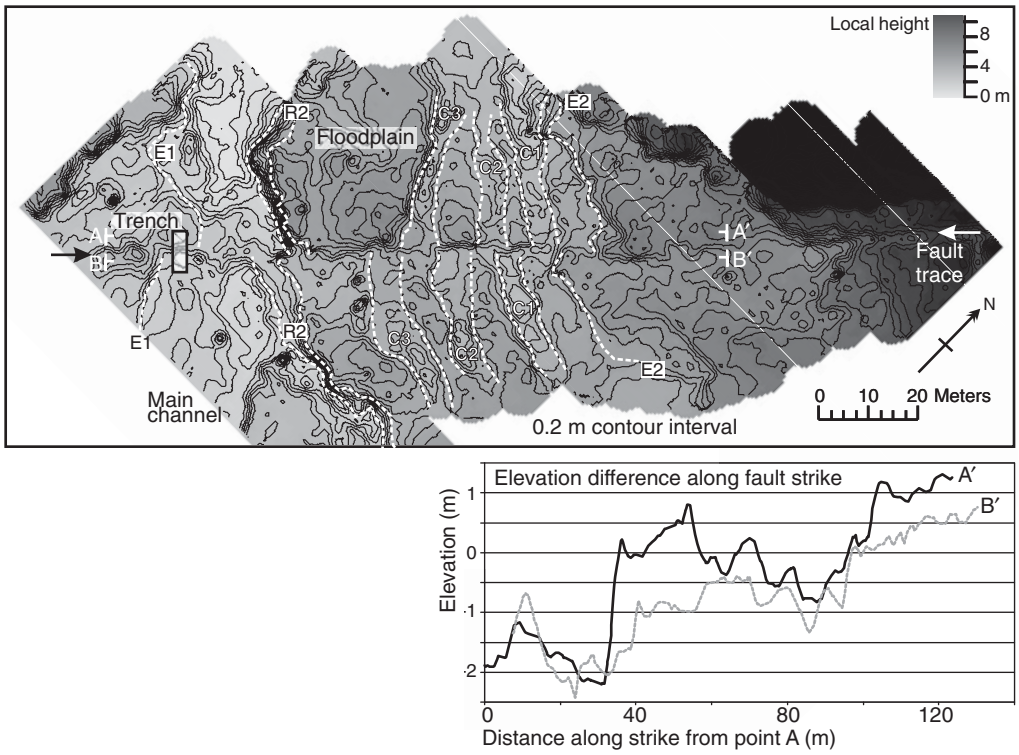

Figure 11. Upper figure shows the microtopography of the Alpine fault scarp across the abandoned gorge. Dashed white lines show channel edges or terrace risers that were correlated across the scarp to measure the amount of dextral offset. Lower figure shows topographic profiles on either side of the fault scarp, along fault strike. Start and end points A-A′ and B-B′ are shown on the contour map above. For comparison, line B-B′ has been shifted horizontally by 7.5 m (the amount of dextral movement in the last earthquake) so that equivalent surfaces approximately match up. This indicates that the vertical offset in the last earthquake was between 0.5 m and 1.5 m; this variation in vertical offset along fault strike is typical of strike-slip faults.

the former floodplain is offset by 7 m. Given uncertainties related to the measurement of channel edges (they vary from 3.5 to 7.5 m), the most reliable offset measurements across the 10 offset features are 7.3–7.6 m. The average is 7.5 ± 1 m. The vertical offset is more difficult to measure because of mismatched surfaces on either side of the fault and some push-up bulges that have formed along the fault (Fig. 11). The best estimate of vertical displacement is 1 ± 0.5 m, up to the northwest.

The 7.5 ± 1 m offset is most likely to be the result of a single rupture, and this was probably the most recent earthquake. We do not see evidence for 17 m of cumulative offset in the abandoned gorge as described by Sutherland and Norris (1995). The most recent earthquake must have occurred after the gorge was abandoned by Hokuri Creek; otherwise, the scarp across the former main channel and the offset edges would have been eroded and trimmed by the river. No suitable material for dating the scarp was found. Since the last earthquake on the Alpine fault in A.D. 1717 ruptured south (near John O'Groats swamp; Cooper and Norris, 1990) and north of Hokuri (Berryman et al., 2012a), we assume that the 7.5 m offsets are the result of this earthquake.

DISCUSSION

The Origin of Cyclical Silt-Peat Sequences at Hokuri

We propose that quasi-periodic surface rupture of the Alpine fault caused the cyclic stratigraphy at Hokuri, with each peat-silt contact representing a large earthquake. This scenario will be fully explained and tested in the following section, where we also consider whether climate or floodplain processes could have controlled the peat-silt sedimentation patterns.

The paleoenvironmental record of the Hokuri sequence shows that, for most of its history, the sedimentary basin was alternating between wetland and very shallow pond environments. Four geomorphic and hydrologic conditions were required for the Hokuri sequence to form (Table 2):

(1) Accommodation space: A shallow sedimentary basin must have persisted for at least

TABLE 2. CRITERIA USED TO IDENTIFY THE MOST LIKELY PROCESS THAT CONTROLLED THE DEVELOPMENT OF THE HOKURI CREEK SEDIMENTARY SEQUENCE

Process:	Fault rupture	Climatic control (storms)	Fluvial processes, channel avulsion
Criteria			
Accommodation space	Y	N	N
Continuous sedimentation	Y	Y	Y
Shallow-water environment maintained	Y	N	Y
Isolation from gravel bed of Hokuri Creek	Y	Y	N

Geological Society of America Bulletin, published online on 22 February 2013 as doi:10.1130/B30693.1

9000 yr, with incremental generation of accommodation space sufficient for 18 m of sediment to accumulate.

(2) Continuous sedimentation: Radiocarbon ages indicate that sedimentation was generally continuous and basinwide. No long hiatuses were identified, and unconformities are rare and not laterally extensive.

(3) Shallow-water sedimentation: A relatively restricted range of water depths was maintained for >18 m of sedimentation. There are no well-developed soils in the Hokuri sequence, indicating that the site was never above the water table for hundreds of years. Only a few beds suggest water depths greater than ~2 m.

(4) Isolation from the main channel of Hokuri Creek: The exposed part of the sedimentary basin was largely isolated from the gravel bed load of Hokuri Creek. At present, Hokuri Creek has a gravel bed, and pits on the former channel in the abandoned gorge show a cobble gravel substrate. Therefore, Hokuri Creek had a gravel bed while the silt-peat sequences were being deposited, and the basin received only the suspended sediment load of the stream, or locally derived sediment.

Scenario 1: Fault Rupture as a Control on Hokuri Basin Stratigraphy

In the fault-rupture scenario, the Hokuri basin would have been a stable, shallow wetland adjacent to the Hokuri Creek floodplain that, near the end of the interseismic period, was accumulating mostly autochthonous organic sediments (Fig. 12). The main channel, with its gravel bed load, was flowing through the gorge. Across the

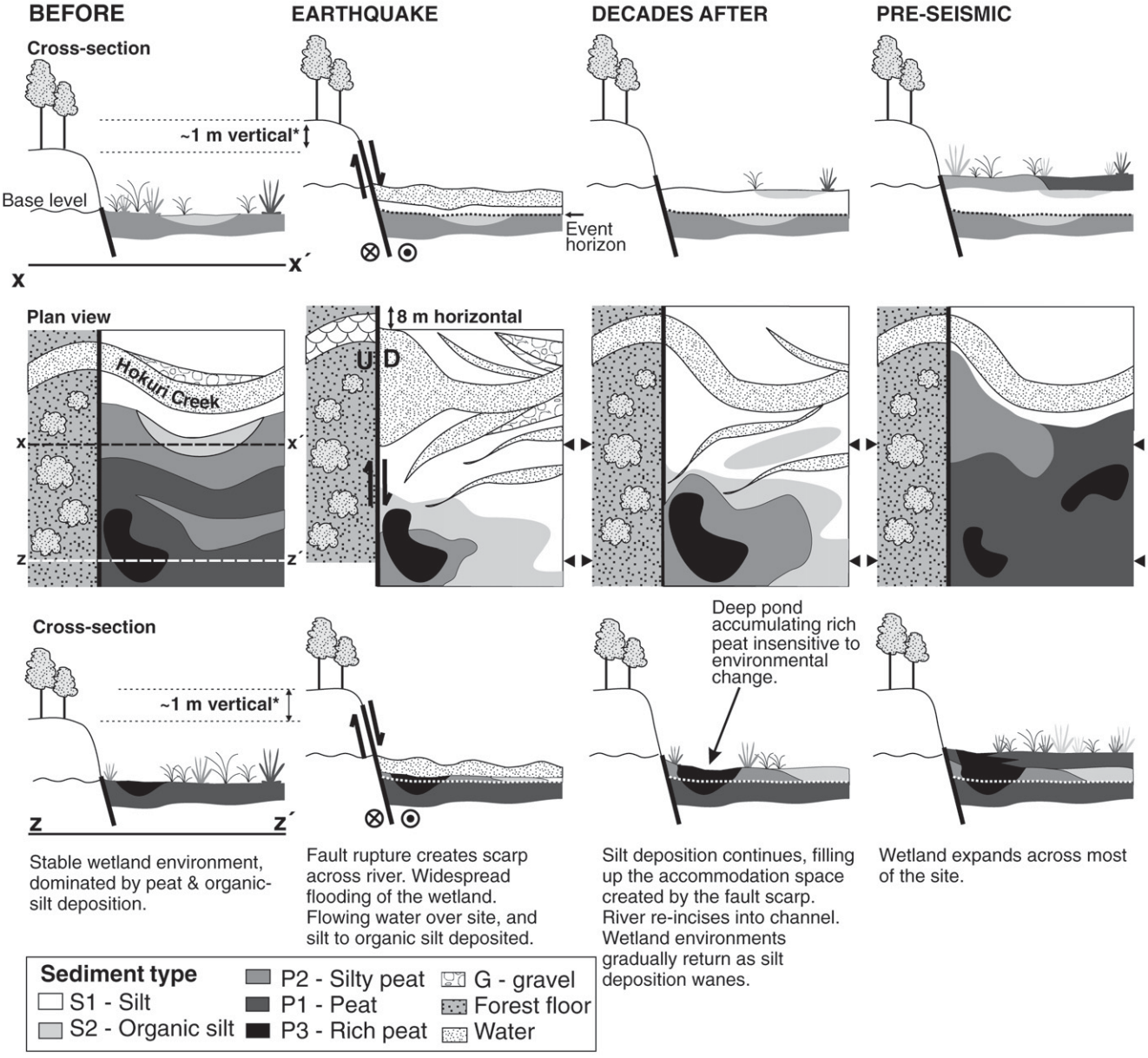

Figure 12. Sketch illustrating the inferred development of the cyclic, fault-rupture–driven, sedimentary sequence at Hokuri Creek. Upper panel shows a cross section of the typical sedimentary sequence. The middle panel shows a plan view of the Hokuri basin. The lower panel shows a cross section of a part of the Hokuri basin that has greater variability in facies. For example, it shows a deep pond that is not affected by the fault rupture. *The west side of the fault is upthrown relative to the east.

Geological Society of America Bulletin, published online on 22 February 2013 as doi:10.1130/B30693.1

Hokuri basin, peat beds developed in shallow, standing water. Thin (centimeter to millimeter scale) silt layers within the peat beds probably represent the suspended sediment load from overbank flood deposits.

A modern analogue for this preseismic environment exists at John O'Groats wetland, 20 km southwest of Hokuri (Figs. 1B and 13). The John O'Groats wetland is on the southern side of where the John O'Groats River meets the Alpine fault scarp. The wetland ranges from small ponds with 0.1–0.3 m depth of standing water closest to the fault, to moss fields and rush land further back, and scrub at the wetland margins (Fig. 13). The wetland has a meandering network of small channels with slowly flowing water ~0.2 m deep. John O'Groats wetland demonstrates that fault scarps are effective impediments to river drainage, even in this high-rainfall environment. It also shows that within a small wetland, there are spatial variations in the type of vegetation and depth and flow of water, and that a river carrying a coarse bed load can be effectively isolated from a neighboring wetland.

Major earthquakes on the Alpine fault had two main impacts on Hokuri Creek and its catchment: (1) NW-side-up and dextral fault rupture across the gorge partially or fully blocked the stream and raised the base level of the stream, and (2) the landscape was destabilized, and sediment supply to the Hokuri Creek basin increased. Fault rupture is marked in the sedimentary record by an abrupt contact between the peat-dominated and silt-dominated beds.

Holocene surface ruptures of the Alpine fault caused relative uplift of the northwestern fault block in the vicinity of Hokuri Creek. Northwestern block uplift is demonstrated by the scarp of the most recent fault rupture across the abandoned gorge (Fig. 11), and early Holocene shell beds on the shores of Lake McKerrow (Fig. 1C) verify long-term uplift to the northwest (Hull and Berryman, 1986; Sutherland and Norris, 1995). Dextral movement of the fault would also have decreased the channel width of Hokuri Creek and restricted water flow through the gorge. For example, the last rupture offset the 20-m-wide main channel bed by ~7.5 m, an ~38% decrease in channel width. Overflow channels on the higher floodplain surface in the abandoned gorge had a width less than the amount of dextral offset in the last earthquake. Therefore, if there had still been flow through the gorge, the overflow channels would have been completely blocked due to dextral displacement alone.

At Hokuri, the combined effect of river blockage and increased sediment supply at the time of and immediately after a major earthquake resulted in flooding of the wetland and a change to a delta-type environment (Fig. 12). Raising the local base level of the stream during fault rupture would have decreased the stream gradient, with consequent effects on channel avulsion, flow speed, and the zones of sediment entrainment and deposition. As the stream approached the fault scarp, flow velocity would have decreased, causing deposition of a higher proportion of the suspended sediment load. New channels would have formed across the river floodplain to distribute this sediment (Fig. 12).

Sediment in the silt beds was probably derived from earthquake-triggered slope destabilization in the Hokuri Creek catchment. Widespread landsliding triggered by large earthquakes has been observed in recent subduction earthquakes in the Fiordland region (Fry et al., 2010; Power et al., 2005), in several historic earthquakes in New Zealand (Hancox et al., 2002), and globally (e.g., Jibson et al., 2006; Keefer, 1994; Koi et al., 2008; Mikos et al., 2006). Earthquake-triggered landslides increase river sediment discharge, with the reported effects lasting from years to decades (e.g., Dadson et al., 2004; Korup et al., 2004; Yanites et al., 2010). Studies along the west coast of the South Island have related pulses of floodplain aggradation and sand dune formation episodes to past Alpine fault earthquakes, consistent with high sediment mobility after major earthquakes (Cullen et al., 2003; Wells and Goff, 2007).

It is unlikely there was any significant time delay between fault rupture and sedimentary change in the Hokuri basin. Flooding of the Hokuri basin due to fault scarp damming probably occurred within hours to days of the earthquake. However, the influx of sediment may have been delayed until a flood mobilized the loosened sediment. For example, following the 1999 Chi-Chi earthquake (Taiwan), there were extensive landslides, but only 8% of the landslides delivered sediment directly to the rivers; the downslope transport of sediment occurred in later typhoons (Dadson et al., 2004). In Taiwan, the period of enhanced sediment yield lasted ~6 yr before returning to pre-earthquake levels (Hovius et al., 2011). Therefore, widespread silt deposition in the Hokuri basin was probably associated with the next large, post-earthquake flood to affect the Hokuri catchment. Given the high rainfall of South Westland (6–7 m/yr), significant floods occur frequently, and we suggest that the influx of silt would have occurred within several months to years of fault

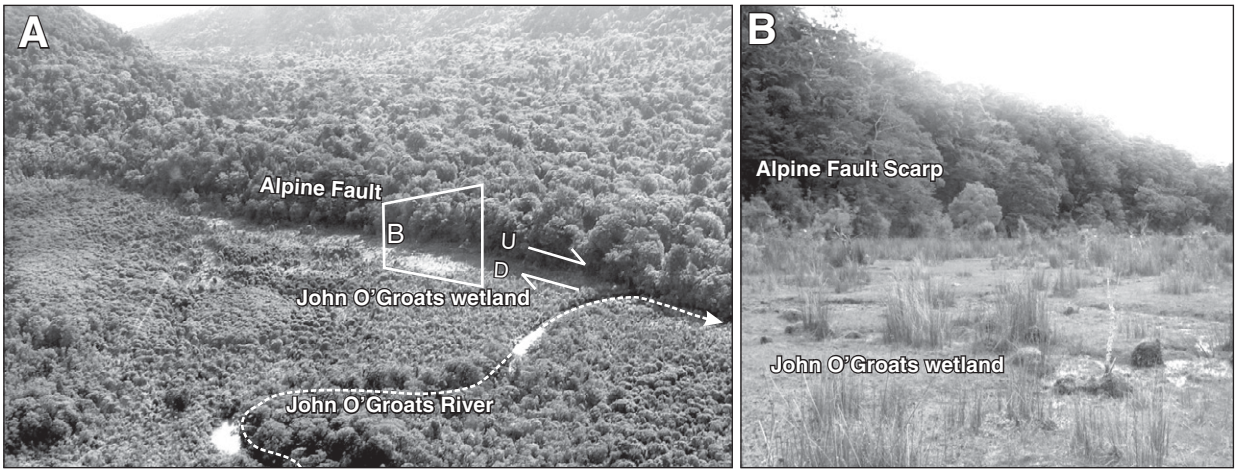

Figure 13. Photos of John O'Groats wetland, a modern analogue to the interseismic environment of the Hokuri basin. The John O'Groats wetland is located 20 km southwest along the Alpine fault from Hokuri Creek (shown on Fig. 1B). John O'Groats River has a right-lateral bend and runs along the fault scarp for 200 m before crossing the fault.

Geological Society of America Bulletin, published online on 22 February 2013 as doi:10.1130/B30693.1

rupture. Such a small time delay is insignificant within the uncertainties of radiocarbon dating. Therefore, we treat the date of the peat-to-silt contact, estimated from closely bracketing radiocarbon ages, as a good estimate of the time of the earthquake.

During the interseismic period, the basin would return to a stable wetland accumulating peat. The timing of the silt to peat transition may have been synchronous across the basin, but it is more likely to have been time transgressive, with silt deposition gradually diminishing in extent. The radiocarbon data do not resolve this (Fig. 8), and it is not important in terms of dating earthquakes. The transition from a silt-dominated sedimentary environment back to a peat-forming wetland may have been controlled by sediment flux or, most likely, by the stream reaching base-level equilibrium.

To reestablish stream base level, either Hokuri Creek had to erode through the fault scarp and incise a channel into the uplifted (northwestern) fault block, or the stream had to build up sediment on the downthrown (southeastern) side of the fault. The sedimentary sequence of the Hokuri basin is evidence that the dominant mechanism of attaining base-level equilibrium was sediment deposition southeast of the fault. Once Hokuri Creek was freely flowing through the gorge and incised sufficiently within its channel, silt transport to the Hokuri basin waned. The wetland could reestablish itself, and autochthonous organic sedimentation became dominant again. The peat beds accumulated over decades to a couple of hundred years. This cycle then restarted with another surface rupture of the Alpine fault.

Returning to the four key criteria for a controlling mechanism for the Hokuri sequence, the fault-rupture model satisfies all of these (Table 2). Accommodation space is incrementally maintained with each fault rupture. The maintenance of accommodation space allows continuous sedimentation across the site, while earthquake-triggered slope destabilization renews the sediment sources. Meter- to decimeter-scale changes in stream base level through each seismic cycle sustain the shallow-water environments over thousands of years.

In the fault-rupture model, the gravel bed load of Hokuri Creek either remains within the main channel of Hokuri Creek or was deposited further upstream from the present Hokuri basin outcrops. The latter is more likely, because the sediment transport capability of Hokuri Creek would have decreased due to diminishing flow speeds as the stream encountered the refreshed fault scarp barrier. Some evidence for an upstream gravel deposition zone is seen from section A, which is dominated by cobble to pebble gravels (Figs. 1D, 2E, and 3). Radiocarbon ages ca. 2000 yr B.C. from an organic silt bed within the gravels indicate that gravel packages were accumulating upstream at the same time that the silty Hokuri basin sequence was accumulating downstream (Fig. 8).

Further affirmation of the fault-rupture scenario comes from comparing the timing and recurrence interval of the peat-to-silt contacts at Hokuri with what is known about the history of the Alpine fault. The most recent peat-to-silt contact occurred at Hokuri at A.D. 730–921. This coincides with the oldest earthquake recorded in paleoseismic trenches at Haast, which has an age range of A.D. 688–1066 (Berryman et al., 2012a). Taking the late Quaternary slip rate of the southern Alpine fault of 23 ± 2 mm/yr (Sutherland et al., 2006) and a single-event displacement of 7.5 ± 1 m (Fig. 9), we find a recurrence interval estimate of 404–260 yr. This is similar to the average recurrence interval of the peat-to-silt contacts at Hokuri of ~330 yr.

Scenario 2: Climatic Control on Cyclic Stratigraphy

An alternative explanation for the cyclic stratigraphy of the Hokuri sedimentary sequence is climatic control of the sedimentation. Large floods or prolonged periods of storminess would provide a means of transporting significant quantities of silt onto a floodplain wetland. The silt influx could overwhelm the wetland flora, and a sharp contact between the peat and silt packages would be created. Furthermore, flood events could potentially inundate the whole Hokuri basin at the same point in time, thereby accounting for the widespread and synchronous change across the basin.

Incompatibilities with the climate-control scenario arise when the interplay between accommodation space and the maintenance of a shallow-water environment is considered (Table 2). If gradual accommodation space increase due to fault rupture is not invoked, then an 18-m-deep basin (the vertical span of the Hokuri sediments) had to exist at the start of the silt-peat accumulation phase. If an 18-m-deep basin existed from the start, then the basin should either have been infilled rapidly (probably within a few flood episodes, assuming sediment supply was not limited), or the sediments should show a gradational paleoenvironmental sequence from deep lake sedimentation initially through to marsh surface at the top. Neither of these options fits with the age and paleoenvironmental data of the Hokuri sequence.

A further possibility is that fault rupture incrementally increased basin accommodation space but had no impact on the sedimentology of the wetland, which was instead controlled by climate. This model cannot be fully dismissed, although several lines of evidence suggest it is unlikely:

(1) Diatoms indicate that the silt packages were deposited in a low-energy environment. In contrast, we would expect storms to trigger sediment deposition in turbulent floods, so that diatoms would be absent from the sediments or be a chaotic assemblage in low abundance.

(2) If each silt package was initiated by an extreme storm, then this implies only 22 such events occurred in the period from A.D. 800 to 6000 B.C. This is a low frequency compared with other New Zealand storm records (e.g., Griffiths and McSaveney, 1983; Orpin et al., 2010; Page et al., 2010).

(3) There is no correlation between the peat-to-silt contacts and published proxies of paleoprecipitation (Fig. 14). If the silt packages of Hokuri were related to storminess or increased precipitation, then the start of silt accumulation should roughly coincide with the start of higher precipitation. The $\delta^{13}C$ record of speleothems (Williams et al., 2004), carbon isotope signatures of fjord sediments (Knudson et al., 2011), palynological records from wetlands (Li et al., 2008; Wilmshurst et al., 2002), and glacier advances in the Southern Alps (Schaefer et al., 2009) can be used as approximate proxies for paleoprecipitation, even though in detail they can be affected by other factors (Fig. 14). Lorrey et al. (2008) summarized speleothem, pollen, and other paleoclimate data sets to identify wet, normal, and dry periods in the western South Island over the past 4000 yr (Fig. 14). The records of paleoprecipitation proxies from southwestern South Island bear no consistent relationship to the timing or frequency of silt-peat contacts at Hokuri (Fig. 14), suggesting that the Hokuri sedimentary sequence was not climate controlled.

(4) If storms controlled sedimentation in Hokuri basin, we would expect more variability in the basin water depth. Some storms may fill the basin with sediment, leaving no room for peat accumulation; some may underfill the basin, allowing deep-water sedimentation; while others might fill the basin above base level, resulting in a period of nondeposition or soil development. Such variability is not seen, suggesting that stream base level controlled basin sedimentation, rather than sediment influx.

We conclude that periods of storminess and/or increased rainfall were probably not the main factors controlling the sedimentary sequence at Hokuri. Extreme rainfall events probably had an impact on the development of the Hokuri sequence at smaller stratigraphic level than the dominant decimeter-scale silt-peat couplets. We suggest that the signature of storms is likely to

Geological Society of America Bulletin, published online on 22 February 2013 as doi:10.1130/B30693.1

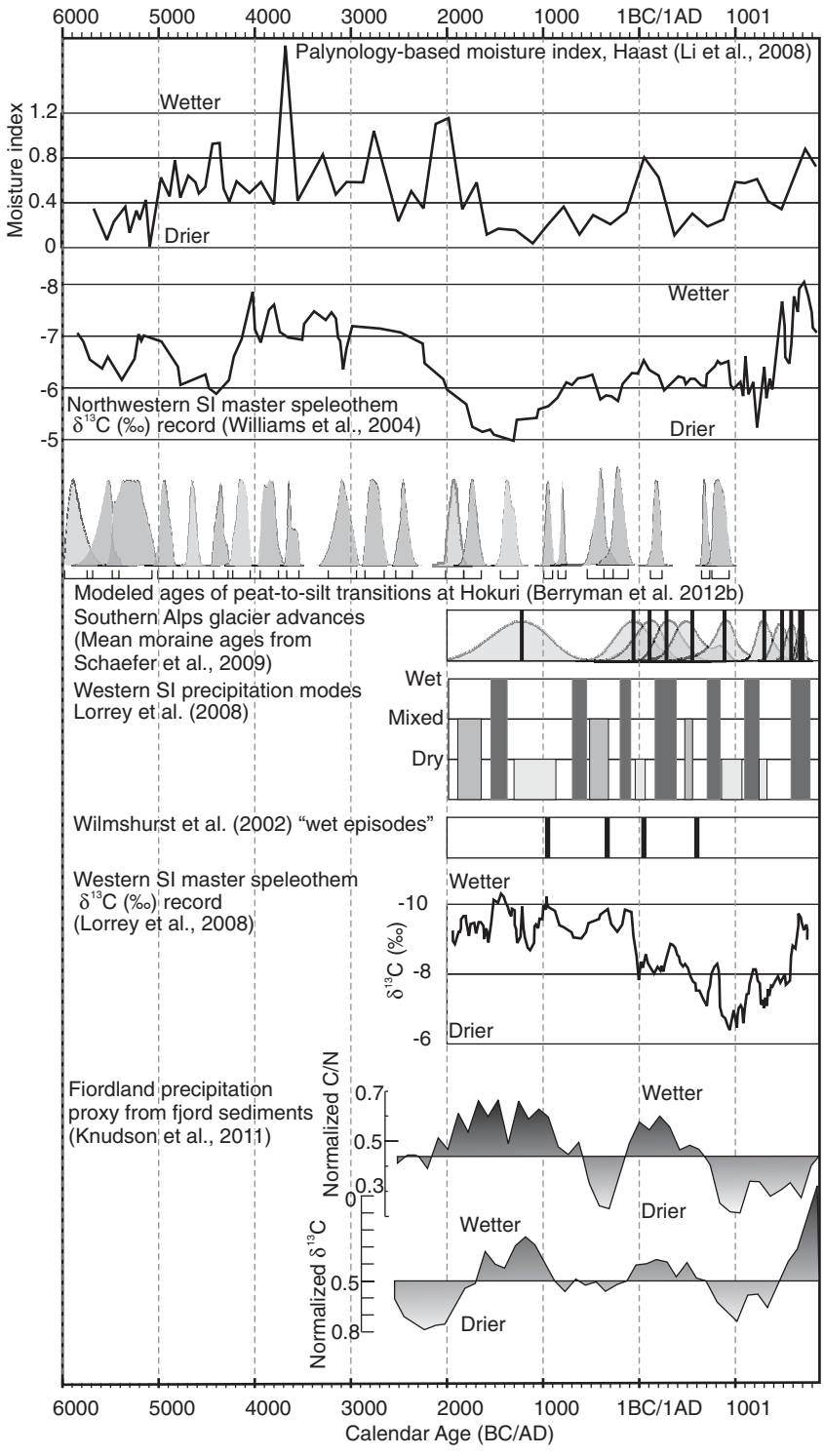

Figure 14. Comparison between the chronology of the peat-to-silt contacts at Hokuri and various Holocene paleoclimate proxies from the South Island (SI; Wilmshurst et al., 2002; Williams et al., 2004; Lorrey et al., 2008; Li et al., 2008; Schaefer et al., 2009; Knudson et al., 2011). This shows that the timing of silt deposition events at Hokuri does not correlate to known climatic signals; we infer that the peat-to-silt contacts are not caused by periods of higher precipitation and storminess.

be the centimeter to millimeter beds of silt seen throughout the sequence (Fig. 15). The silt beds are particularly obvious within the peats beds due to the color contrast, but they also occur as particularly pale laminae within silt beds. They tend to have an irregular pattern, with an estimated average of 3–5 silt beds (millimeter- to centimeter-scale) per century, a rate more compatible with an extreme storm record (cf. Lake Tutira record, Page et al., 2010).

Scenario 3: Floodplain Processes

Could the decimeter-scale peat-silt alternations in the Hokuri sequence be due to floodplain aggradation processes? Floodplains are dynamic environments, particularly so in Fiordland with its high annual rainfall (up to 7 m/yr) and mountainous relief. The most likely process is by channel avulsion, which is the abandonment of all or part of a channel in favor of a new course. Abrupt peat-to-silt contacts have been observed on many floodplains that undergo channel avulsion (e.g., Davies-Vollum and Kraus, 2001; Makaske et al., 2007; Slingerland and Smith, 2004; Smith et al., 1989; Smith and Perez-Arlucea, 1994). Such stratigraphy develops as wetlands that exist behind natural levees on the low parts of floodplains are inundated by the main flow of the channel due to avulsion. The avulsion redistributes bed load and suspended sediment. After a period of time, the new channel will entrench, and the floodplain will stabilize, therefore allowing peat to form again.

Channel avulsions can occur instantaneously or gradually, and thus the peat-to-silt transition could be synchronous or diachronous, and they can occur at widely varying recurrence intervals. Slingerland and Smith (2004) give examples of avulsions with recurrences of 28 yr up to 1400 yr, while Stouthamer and Berendsen (2001) document avulsion frequencies on the Rhine-Meuse delta that vary through the Holocene from 41 to 117 yr. Thus, the recurrence of avulsions could be comparable to the Hokuri peat-to-silt contact frequency. The degree to which the paleo–Hokuri Creek would have been susceptible to avulsion is difficult to evaluate because the current stream gradient is different to what it would have been when it flowed through the gorge. In any case, the valley was probably still quite narrow, leaving only a small width for an avulsing channel system.

The initiation of avulsion is typically described as two phases: the setup and the trigger (Mohrig et al., 2000; Slingerland and Smith, 2004). The setup phase sees the river aggrade within its channel, so that it is perched above its floodplain, and then a trigger event creates a failure in the natural levee, which initiates

Geological Society of America Bulletin, published online on 22 February 2013 as doi:10.1130/B30693.1

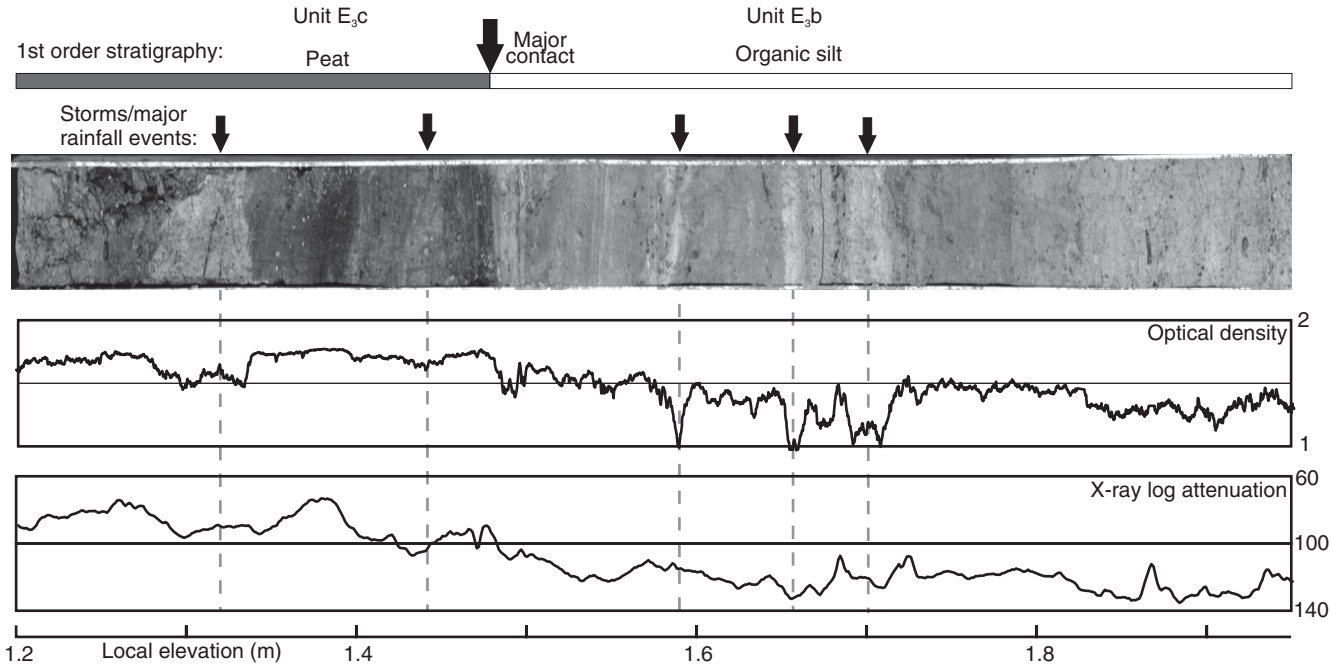

Figure 15. A section of core from the E_3 section demonstrating the different scales of the sedimentary beds. At decimeter scale, there are peat and silt beds, but at a centimeter to millimeter scale, there are silt beds that probably represent individual storm deposits.

the avulsion. Triggers for avulsion are typically floods, but landslides and tectonic events can also trigger avulsions (e.g., Guccione et al., 2002; Korup, 2004). In the Hokuri paleoenvironment, floods and earthquakes would be the obvious triggers of avulsion.

Avulsion processes would allow continuous sedimentation across the Hokuri basin, and they may be compatible with the maintenance of a shallow-water environment, satisfying two of the criteria for sequence development (Table 2). However, a higher occurrence of unconformities due to channel scouring would be expected for avulsion and probably more variability in water depth due to the topographic relief required across a floodplain in order for avulsion to occur.

One likely candidate for a channel avulsion event is the 2–3-m-thick gravel bed that outcrops at the base of section B and the top of section E_4, but otherwise there is little evidence that channel avulsion was a typical occurrence at Hokuri Creek. The avulsion process on its own does not create accommodation space over time, and it would not effectively isolate the gravel bed load of Hokuri Creek from the Hokuri sedimentary basin (Table 2).

To conclude, channel avulsion is unlikely to be the main process responsible for the decimeter-scale silt-peat alternations of the Hokuri sequence. The reasonably uniform silt-peat couplets are inconsistent with the more variable and lens-like architecture of avulsion sequences, and the absence of widespread gravel indicates that the main channel rarely left its preferred path. While repeated avulsions can occur, an increase in accommodation space is required so that subsequent channel avulsions do not scour and rework the existing floodplain sediments. Thus, channel avulsion triggered by an earthquake might have occurred occasionally, but as an isolated process, channel avulsion was not the main control on development of the Hokuri sequence.

A Long Paleoseismic Record on the Alpine Fault

We conclude that repeated fault rupture is the most likely process to have caused the deposition of the decimeter-scale silt-peat couplets of the Hokuri sequence. Spanning ~7000 yr, the Hokuri sequence represents one of the longest and most complete records of paleoearthquakes in the world. Therefore, it is important to consider the completeness of our interpretation of the record.

Have We Overestimated the Number of Earthquakes at Hokuri?

Inferred earthquakes could be overestimated in the Hokuri sequence if some of the peat-to-silt contacts were caused by processes other than Alpine fault ruptures. As already mentioned, potential causes of non–fault rupture couplets could be extreme rainfall events, nontectonic catchment disturbances, or non-Alpine fault earthquakes that destabilized the Hokuri catchment. A few couplets may possibly be storm related, but the fact that the sequence is fine grained rather than coarser, poorly sorted, and highly variable in space, provides a strong basis for ruling out this possibility.

Large landslides unrelated to earthquakes or extreme rainfall may have occurred in the Hokuri catchment during the Holocene (e.g., the 1999 Mount Adams rock avalanche had no obvious seismic or rainfall triggers; Hancox et al., 2005). However, large landslide scars or remnant debris piles within the catchment have not been observed.

Ground shaking by regional earthquakes (i.e., Skippers Range fault or the northern end of the Puysegur subduction zone; Fig. 1) could also have caused influx of sediment to Hokuri Creek. The paleoseismic history of the Skippers Range fault is unknown, although the presence of a scarp across mountaintops that were glaciated in the last glacial stage suggests that there has been at least one postglacial rupture. Therefore, Holocene rupture of the Skippers Range fault cannot be ruled out, but it was probably a rare occurrence in comparison to Alpine fault rupture. Large earthquakes on the Puysegur subduction zone are known to trigger widespread landsliding, but comparisons with recent subduction earthquakes (1993, 2003, 2007, and 2009; Hancox and Cox, 2010; Hancox et al., 2003;

Van Dissen et al., 1994) suggest that the Hokuri catchment is not very susceptible to shaking from Puysegur subduction zone earthquakes.

In summary, there are some reasons why the peat-to-silt contacts may overestimate the number of Alpine fault earthquakes, but none of these is compelling. The uniformity of the silt-peat couplets suggests that the same process is occurring repeatedly, rather than several different processes producing surprisingly similar stratigraphy.

Have We Underestimated the Number of Earthquakes at Hokuri?

The completeness of the Hokuri earthquake record relies on every surface-rupturing earthquake resulting in a peat-to-silt contact. Could the sequence be missing large surface-rupturing earthquakes on the Alpine fault? Erosion is one mechanism for removing evidence of earthquakes, but there are no recognized large unconformities in the Hokuri sequence. Where there are local unconformities, radiocarbon dating suggests that complete sequences are observed in nearby outcrops.

Large earthquakes might not be recorded by the Hokuri stratigraphy if no coseismic surface rupture occurred. The relationship between surface rupture and magnitude is variable (Wells and Coppersmith, 1994), but, in general, earthquakes of ~M > 6.5 on strike-slip faults produce surface ruptures. The locking depth of the Alpine fault is relatively shallow at 6–12 km (Sutherland et al., 2007), so the nucleation of large, deep earthquakes that do not rupture the surface is unlikely. It is probable that past large (M > 7) earthquakes on the Alpine fault produced surface rupture and are potentially recorded by the Hokuri sequence. Small- to moderate-magnitude earthquakes that did not rupture the surface are unlikely to be recorded in the sequence because non-surface-rupturing earthquakes would not produce any new accommodation space.

Surface-rupturing earthquakes on the Alpine fault at Hokuri Creek might not be recorded if the paleoenvironment at the time of the earthquake was insensitive to an ~1 m change in stream base level, or if part of the basin was already dominated by silt deposition prior to the earthquake. This was certainly the case for some events in some parts of the basin (e.g., Hk8 and Hk15, discussed previously), but we suggest only one event (Hk10) was not recorded by a distinct stratigraphic change anywhere in the basin. Hk10 is not expressed by a clear sedimentological change but has some paleoecological support; hence, we have included it as an event in our earthquake chronology. Without event Hk10, the time interval between Hk11 and Hk9 is the longest inter-vent interval in the whole Hokuri basin sequence, at 660 ± 225 yr. Including Hk10 reduces that recurrence interval to a value more comparable with the average for the rest of the sequence, which, including event Hk10 is 329 ± 68 yr.

Other than Hk10, we do not identify any other potential locations within the Hokuri sequence where missing events may lie. Some individual sections are missing events, and this is to be expected given the environmental variability seen within wetlands (e.g., compare with John O'Groats swamp; Fig. 13). In some places, wetland ponds could have been too deep to significantly change in response to a rise in stream base level. An example of this is bed H_1g (correlates to Ia), which is a rich, dark peat that accumulated over 950 yr. Age correlations imply that this peat bed spans two earthquakes that are expressed stratigraphically in nearby outcrops. Likewise, there were parts of the Hokuri basin that were dominated by silt deposition and did not fully revert to wetland conditions between earthquakes. The lateral loss of definition of the Hk8 contact toward section E_1 is an example of this (Fig. 8).

Implications of Developing Long Earthquake Records from Near-Fault Sedimentary Basins

The Hokuri study demonstrates that long earthquake records can be extracted from sedimentary sequences immediately adjacent to faults due to the intimate relationships among the fault scarp, drainage, and sedimentation. Fluvio-wetland sedimentary sequences next to major faults have long been used as recorders of paleoearthquakes (e.g., on the San Andreas fault; Sieh, 1978; Weldon et al., 2002) because such sequences can contain organic material for radiocarbon dating and near-continuous sedimentation. However, studies such as those cited here typically use direct structural relationships between stratigraphic horizons and fault tip terminations to identify paleoearthquakes. The Hokuri study uses paleoenvironmental changes in a fault-adjacent basin as evidence of earthquakes. Stratigraphic horizons extend close to the Alpine fault scarp, but offsets are not observed directly on fault planes. The main advantage of using near-fault sedimentary basin sequences such as Hokuri, rather than on-fault sedimentary sequences, is that evidence of older earthquakes is preserved and suffers no overprinting by recent earthquakes.

Given the rarity of long earthquake records worldwide, and their exceptional value in understanding fault behavior, we consider the paleogeographic conditions that made this study possible. The upstream-facing fault scarp meant that fault rupture contributed to basin formation and changes in hydrologic regime. Accumulation of fine-grained sediment through the interseismic and coseismic intervals allowed identification of subtle stratigraphic and paleoenvironmental changes, and continuity of sediment deposition lessened the potential for not recording paleoearthquakes. Abundant dateable material throughout the sequence, and crucially, bracketing the event horizon, was a major benefit. Multiple and widely spread outcrops facilitated the identification of missing events, and sampling from throughout the basin increased the likelihood of attaining a complete record. Paleoecological studies were crucial for providing a more complete understanding of the past environment, as well as the changes taking place at event horizons.

There is no reason why near-fault sequences similar to Hokuri would not be preserved in other locations, both along the Alpine fault, and on other faults globally. There are many cases where streams cross upstream-facing scarps, although there are probably fewer cases where the stream has diverted and then incised extensive exposures. Nevertheless, a closely spaced coring campaign would probably have success in obtaining near-fault sedimentary basin sequences in cases where natural incision has not occurred.

The exceptionally well-dated, long earthquake record extracted from Hokuri enables the time-dependent fault behavior to be tested. This was discussed in the study by Berryman et al. (2012b), in which the Hokuri record was merged with the three most recent surface-rupturing earthquakes from Haast to obtain a record of the past 24 major earthquakes on the southern Alpine fault. The mean recurrence interval is 329 ± 68 yr (standard error), and the coefficient of variation in recurrence interval is 0.33. Therefore, earthquake recurrence on the Alpine fault is quasi-periodic. In comparison with long earthquake records on other major faults such as the San Andreas fault (Scharer et al., 2010) and Dead Sea Transform (Ferry et al., 2011; Marco et al., 1996), the Alpine fault exhibits some of the most periodic recurrence behavior so far documented. This quasi-periodic recurrence behavior is largely attributed to its isolation from other major faults, its high slip rate, and its simple structure (a mature fault with few stepovers that is smooth at seismogenic depth; Berryman et al., 2012b).

CONCLUSIONS

A predominantly shallow-water sedimentary sequence accumulated against the scarp of the

Alpine fault at Hokuri Creek, providing an exceptional record of cyclical paleoenvironmental change associated with large earthquakes. Surface rupture of the Alpine fault would have fully to partially blocked Hokuri Creek and destabilized hillslopes of the catchment. Therefore, earthquakes created a change in stream base level, enhancing deposition on the downthrown side of the fault at the same time that sediment supply increased. Peat-dominated wetlands on the Hokuri Creek floodplain were rapidly "drowned" by an influx of silt immediately following each earthquake. The sharp and basinwide peat-to-silt contacts thus represent fault ruptures.

This record of fault-controlled sedimentation at Hokuri Creek is remarkable for its continuity, the number of earthquakes recorded, and the high-resolution dating. A key advantage of near-fault sedimentary basins like Hokuri is that evidence of older earthquakes is not overprinted by recent earthquakes, an attribute that was essential for developing the long earthquake record at Hokuri Creek. Long paleoearthquake records are needed to understand fault behavior, given that the historic and instrumental records of earthquakes are generally too short to assess the variability in earthquake cycles. The Hokuri paleoearthquake record has already made a significant contribution to understanding the earthquake recurrence behavior of the Alpine fault (Berryman et al., 2012b), and in the future it will contribute to assessing the seismic hazard, constraining rupture lengths of large earthquakes, and understanding how the landscape responds and reestablishes equilibrium following large earthquakes.

ACKNOWLEDGMENTS

This project was funded by the Royal Society of New Zealand Marsden fund. We would like to acknowledge colleagues who assisted in the field or in the laboratory: Neville Palmer, Lizzie Ingham, Tom Dutton, John West, Marianna Terezow, and Bernard Barry. Walter Somerville undertook analysis of the magnetic mineral compositions. Dallas Mildenhall and Liz Kennedy provided valuable feedback in the early stages of this project about the use of palynology. Reviewers Mauri McSaveney, Andy Nicol, and an anonymous reviewer are thanked for their excellent comments on the manuscript.

REFERENCES CITED

Aaby, B., and Berglund, B.E., 1986, Characterization of peat and lake deposits, *in* Berglund, B.E., ed., Handbook of Holocene Palaeoecology and Palaeohydrology: Caldwell, UK, John Wiley & Sons, p. 231–246.

Allen, J.R.L., 1999, Geological impacts on coastal wetland landscapes: Some general effects of sediment autocompaction in the Holocene of northwest Europe: The Holocene, v. 9, p. 1–12, doi:10.1191/095968399674929672.

Barnes, P., 2009, Postglacial (after 20 ka) dextral slip rate of the offshore Alpine fault, New Zealand: Geology, v. 37, no. 1, p. 3–6, doi:10.1130/G24764A.1.

Barnes, P., Sutherland, R., and Delteil, J., 2005, Strike-slip structure and sedimentary basins of the southern Alpine fault, Fiordland, New Zealand: Geological Society of America Bulletin, v. 117, no. 3/4, p. 411–435; doi: 410.1030/B25458.25451.

Berryman, K., Beanland, S., Cooper, A.F., Cutten, H.N., Norris, R.J., and Wood, P.R., 1992, The Alpine fault, New Zealand: Variation in Quaternary structural style and geomorphic expression: Annales Tectonicae, v. VI, supplement, p. 126–163.

Berryman, K., Cooper, A., Norris, R., Villamor, P., Sutherland, R., Wright, T., Schermer, E., Langridge, R., and Biasi, G., 2012a, Late Holocene rupture history of the Alpine fault in South Westland, New Zealand: Bulletin of the Seismological Society of America, v. 102, no. 2, p. 620–638, doi:10.1785/0120110177.

Berryman, K.R., Cochran, U.A., Clark, K.J., Biasi, G.P., Langridge, R.M., and Villamor, P., 2012b, Major earthquakes occur regularly on an isolated plate boundary fault: Science, v. 336, p. 1690–1693, doi:10.1126/science.1218959.

Bronk Ramsey, C., 2001, Development of the radiocarbon calibration program OxCal: Radiocarbon, v. 43, no. 2A, p. 355–363.

Bronk Ramsey, C., 2009, Bayesian analysis of radiocarbon dates: Radiocarbon, v. 51, no. 1, p. 337–360.

Brugam, R.B., McKeever, K., and Kolesa, L., 1998, A diatom-inferred water depth reconstruction for an Upper Peninsula, Michigan, lake: Journal of Paleolimnology, v. 20, p. 267–276, doi:10.1023/A:1007948616511.

Chui, G., 2009, Seismology: Shaking up earthquake theory: Nature, v. 461, p. 870–872, doi:10.1038/461870a.

Cooper, A.F., and Norris, R.J., 1990, Estimates for the timing of the last coseismic displacement on the Alpine fault, northern Fiordland, New Zealand: New Zealand Journal of Geology and Geophysics, v. 33, p. 303–307, doi:10.1080/00288306.1990.10425688.

Cullen, L., Duncan, R., Wells, A., and Stewart, G., 2003, Floodplain and regional scale variation in earthquake effects on forests, Westland, New Zealand: Journal of the Royal Society of New Zealand, v. 33, no. 4, p. 693–701, doi:10.1080/03014223.2003.9517753.

Dadson, S.J., Hovius, N., Chen, H., Dade, W.B., Lin, J.-C., Hsu, M.-L., Lin, C.-W., Horng, M.-J., Chen, T.-C., Milliman, J., and Stark, C.P., 2004, Earthquake-triggered increase in sediment delivery from an active mountain belt: Geology, v. 32, no. 8, p. 733–736, doi:10.1130/G20639.1.

Davies-Vollum, K.S., and Kraus, M.J., 2001, A relationship between alluvial backswamps and avulsion cycles: An example from the Willwood Formation of the Bighorn Basin, Wyoming: Sedimentary Geology, v. 140, no. 3–4, p. 235–249, doi:10.1016/S0037-0738(00)00186-X.

Ferry, M., Meghraoui, M., Karaki, N., Al-Taj, M., and Khahil, L., 2011, Episodic behavior of the Jordon Valley section of the Dead Sea fault inferred from a 14-ka-long integrated catalog of large earthquakes: Bulletin of the Seismological Society of America, v. 101, no. 1, p. 39–67, doi:10.1785/0120100097.

Fry, B., Bannister, S., Beavan, J., Bland, L., Bradley, B., Cox, S., Cousins, J., Gale, N., Hancox, G., Holden, C., Jongens, R., Power, W., Prasetya, G., Reyners, M., Ristau, J., Robinson, R., Samsonov, S., Wilson, K., and GeoNet Team, 2010, The Mw 7.8 Dusky Sound Earthquake of 2009: Preliminary report: Bulletin of the New Zealand National Society for Earthquake Engineering, v. 43, no. 4, p. 24–40.

Goldfinger, C., Nelson, C.H., Johnson, J.E., and Party, S.S., 2003, Holocene earthquake records from the Cascadia subduction zone and northern San Andreas fault based on precise dating of offshore turbidites: Annual Review of Earth and Planetary Science, v. 31, p. 555–577, doi:10.1146/annurev.earth.1131.100901.141246.

Griffiths, G., and McSaveney, M., 1983, Hydrology of a basin with extreme rainfalls—Cropp River, New Zealand: New Zealand Journal of Science, v. 26, p. 293–306.

Guccione, M.J., Mueller, K., Champion, J., Shepherd, S., Carlson, S.D., Odhiambo, B., and Tate, A., 2002, Stream response to repeated coseismic folding, Tiptonville dome, New Madrid seismic zone: Geomorphology, v. 43, no. 3–4, p. 313–349, doi:10.1016/S0169-555X(01)00145-3.

Hancox, G., and Cox, S., 2010, The nature and significance of landslides caused by the Mw 7.6 earthquake of 15 July 2009 in Fiordland, New Zealand, *in* Williams, A.L., Pinches, G.M., Chin, C.Y., McMorran, T.J., and Massey, C.I., eds., Geologically Active: Proceedings of 11th International Association for Engineering Geology and the Environment Congress, Auckland, September 2010: Boca Raton, Florida, CRC Press, p. 219–228.

Hancox, G., Perrin, N., and Dellow, G., 2002, Recent studies of historical earthquake-induced landsliding, ground damage and MM intensity in New Zealand: Bulletin of the New Zealand Society for Earthquake Engineering, v. 35, no. 2, p. 59–95.

Hancox, G., Cox, S., Turnbull, I.M., and Crozier, M.J., 2003, Reconnaissance Studies of Landslides and Other Ground Damage Caused by the Mw 7.2 Fiordland Earthquake of 22 August 2003: Institute of Geological and Nuclear Sciences Science Report 2003/30, 32 p.

Hancox, G., McSaveney, M.J., Manville, V.R., and Davies, T.R., 2005, The October 1999 Mt. Adams rock avalanche and subsequent landslide dam-break flood and effects in Poerua River, Westland, New Zealand: New Zealand Journal of Geology and Geophysics, v. 48, no. 4, p. 683–705, doi:10.1080/00288306.2005.9515141.

Hovius, N., Meunier, P., Lin, C.-W., Chen, H., Chen, Y.-G., Dadson, S., Horng, M.-J., and Lines, M., 2011, Prolonged seismically induced erosion and the mass balance of a large earthquake: Earth and Planetary Science Letters, v. 304, no. 3–4, p. 347–355, doi:10.1016/j.epsl.2011.02.005.

Hull, A., and Berryman, K., 1986, Holocene tectonism in the region of the Alpine fault at Lake McKerrow, Fiordland, New Zealand: Royal Society of New Zealand Bulletin, v. 24, p. 317–331.

Jibson, R.W., Harp, E.L., Schulz, W., and Keefer, D.K., 2006, Large rock avalanches triggered by the M 7.9 Denali fault, Alaska, earthquake of 3 November 2002: Engineering Geology, v. 83, no. 1–3, p. 144–160, doi:10.1016/j.enggeo.2005.06.029.

Keefer, D.K., 1994, The importance of earthquake-induced landslides to long-term slope erosion and slope-failure hazards in seismically active regions: Geomorphology, v. 10, no. 1–4, p. 265–284, doi:10.1016/0169-555X(94)90021-3.

Knudson, K.P., Hendy, I.L., and Neil, H.L., 2011, Re-examining Southern Hemisphere westerly wind behavior: Insights from a late Holocene precipitation reconstruction using New Zealand fjord sediments: Quaternary Science Reviews, v. 30, no. 21–22, p. 3124–3138, doi:10.1016/j.quascirev.2011.07.017.

Koi, T., Hotta, N., Ishigaki, I., Matuzaki, N., Uchiyama, Y., and Suzuki, M., 2008, Prolonged impact of earthquake-induced landslides on sediment yield in a mountain watershed: The Tanzawa region, Japan: Geomorphology, v. 101, no. 4, p. 692–702, doi:10.1016/j.geomorph.2008.03.007.

Korup, O., 2004, Landslide-induced river channel avulsions in mountain catchments of southwest New Zealand: Geomorphology, v. 63, no. 1–2, p. 57–80, doi:10.1016/j.geomorph.2004.03.005.

Korup, O., McSaveney, M.J., and Davies, T.R.H., 2004, Sediment generation and delivery from large historic landslides in the Southern Alps, New Zealand: Geomorphology, v. 61, no. 1–2, p. 189–207, doi:10.1016/j.geomorph.2004.01.001.

Langridge, R., Van Dissen, R., Rhoades, D. A., Villamor, P., Little, T., Litchfield, N., Clark, K., and Clark, D., 2011, Five thousand years of surface ruptures on the Wellington fault, New Zealand: Implications for recurrence and fault segmentation: Bulletin of Seismological Society of America, v. 101, no. 5, p. 2088–2107, doi:10.1785/0120100340.

Li, X., Rapson, G.L., and Flenley, J.R., 2008, Holocene vegetational and climatic history, Sponge Swamp, Haast, south-western New Zealand: Quaternary International, v. 184, no. 1, p. 129–138, doi:10.1016/j.quaint.2007.09.011.

Lienkaemper, J.J., and Williams, P.L., 2007, A record of large earthquakes on the southern Hayward fault for the past 1800 years: Bulletin of the Seismological Society of America, v. 97, no. 6, p. 1803–1819, doi:10.1785/0120060258.

Long, A.J., Waller, M.P., and Stupples, P., 2006, Driving mechanisms of coastal change: Peat compaction and the destruction of late Holocene coastal wetlands: Marine Geology, v. 225, p. 63–84, doi:10.1016/j.margeo.2005.09.004.

Lorrey, A., Williams, P., Salinger, J., Martin, T., Palmer, J., Fowler, A., Zhao, J.-x., and Neil, H., 2008, Speleothem stable isotope records interpreted within a multi-proxy framework and implications for New Zealand palaeoclimate reconstruction: Quaternary International, v. 187, no. 1, p. 52–75, doi:10.1016/j.quaint.2007.09.039.

Makaske, B., Berendsen, H.J.A., and Van Ree, M.H.M., 2007, Middle Holocene avulsion-belt deposits in the central Rhine-Meuse delta, The Netherlands: Journal of Sedimentary Research, v. 77, p. 110–123, doi:10.2110/jsr.2007.004.

Marco, S., Stein, M., Agnon, A., and Ron, H., 1996, Long-term earthquake clustering: A 50,000-year paleoseismic record in the Dead Sea graben: Journal of Geophysical Research, v. 101, no. B3, p. 6179–6191, doi:10.1029/95JB01587.

McCormac, F.G., Hogg, A.G., Blackwell, P.G., Buck, C.E., Higham, T.F.G., and Reimer, P.J., 2004, SHCal04 Southern Hemisphere Calibration, 0–26 ka cal BP: Radiocarbon, v. 46, p. 1087–1092.

Mikos, M., Fazarinc, R., and Ribicic, M., 2006, Sediment production and delivery from recent large landslides and earthquake-induced rock falls in the Upper Soca River Valley, Slovenia: Engineering Geology, v. 86, no. 2–3, p. 198–210, doi:10.1016/j.enggeo.2006.02.015.

Mohrig, D., Heller, P.L., Paola, C., and Lyons, W.J., 2000, Interpreting avulsion process from ancient alluvial sequences: Guadalope-Matarranya system (northern Spain) and Wasatch Formation (western Colorado): Geological Society of America Bulletin, v. 112, no. 12, p. 1787–1803, doi:10.1130/0016-7606(2000)112<1787:IAPFAA>2.0.CO;2.

Moos, M.T., Laird, K.R., and Cumming, B.F., 2005, Diatom assemblages and water depth in Lake 239 (Experimental Lakes Area, Ontario): Implications for paleoclimatic studies: Journal of Paleolimnology, v. 34, p. 217–227, doi:10.1007/s10933-005-2382-8.

Norris, R.J., and Cooper, A.F., 1995, Origin of small-scale segmentation and transpressional thrusting along the Alpine fault, New Zealand: Geological Society of America Bulletin, v. 107, no. 2, p. 231–240, doi:10.1130/0016-7606(1995)107<0231:OOSSSA>2.3.CO;2.

Norris, R.J., and Cooper, A.F., 1997, Erosional control on the structural evolution of a transpressional thrust complex on the Alpine fault, New Zealand: Journal of Structural Geology, v. 19, no. 10, p. 1323–1342, doi:10.1016/S0191-8141(97)00036-9.

Norris, R.J., and Cooper, A.F., 2001, Late Quaternary slip rates and slip partitioning on the Alpine fault, New Zealand: Journal of Structural Geology, v. 23, no. 2–3, p. 507–520, doi:10.1016/S0191-8141(00)00122-X.

Norris, R.J., and Cooper, A.F., 2007, The Alpine fault, New Zealand: Surface geology and field relationships, *in* Okaya, D., Stern, T., and Davey, F., eds., A Continental Plate Boundary: Tectonics at South Island, New Zealand: American Geophysical Union Geophysical Monograph 175, p. 157–175.

Orpin, A.R., Carter, L., Page, M.J., Cochran, U.A., Trustrum, N.A., Gomez, B., Palmer, A.S., Mildenhall, D.C., Rogers, K.M., Brackley, H.L., and Northcote, L., 2010, Holocene sedimentary record from Lake Tutira: A template for upland watershed erosion proximal to the Waipaoa Sedimentary System, northeastern New Zealand: Marine Geology, v. 270, no. 1–4, p. 11–29, doi:10.1016/j.margeo.2009.10.022.

Page, M.J., Trustrum, N.A., Orpin, A.R., Carter, L., Gomez, B., Cochran, U.A., Mildenhall, D.C., Rogers, K.M., Brackley, H.L., Palmer, A.S., and Northcote, L., 2010, Storm frequency and magnitude in response to Holocene climate variability, Lake Tutira, north-eastern New Zealand: Marine Geology, v. 270, no. 1–4, p. 30–44, doi:10.1016/j.margeo.2009.10.019.

Parsons, T., 2008, Earthquake recurrence on the south Hayward fault is most consistent with a time dependent, renewal process: Geophysical Research Letters, v. 35, no. 21, L21301, doi:10.1029/2008GL035887.

Power, W., Downes, G., McSaveney, M., Beavan, J., and Hancox, G., 2005, The Fiordland earthquake and tsunami, New Zealand, 21 August 2003: Tsunamis: Advances in Natural and Technological Hazards Research, v. 23, p. 31–42, doi:10.1007/1-4020-3331-1_2.

Schaefer, J.M., Denton, G.H., Kaplan, M., Putnam, A., Finkel, R.C., Barrell, D.J.A., Andersen, B.G., Schwartz, R., Mackintosh, A., Chinn, T., and Schlüchter, C., 2009, High-frequency Holocene glacier fluctuations in New Zealand differ from the northern signature: Science, v. 324, no. 5927, p. 622–625, doi:10.1126/science.1169312.

Scharer, K.M., Biasi, G.P., Weldon, R.J., II, and Fumal, T.E., 2010, Quasi-periodic recurrence of large earthquakes on the southern San Andreas fault: Geology, v. 38, no. 6, p. 555–558, doi:10.1130/G30746.1.

Sieh, K.E., 1978, Prehistoric large earthquakes produced by slip on the San Andreas fault at Pallett Creek, California: Journal of Geophysical Research, v. 83, no. B8, p. 3907–3939, doi:10.1029/JB083iB08p03907.

Slingerland, R., and Smith, N.D., 2004, River avulsions and their deposits: Annual Review of Earth and Planetary Sciences, v. 32, p. 257–285, doi:10.1146/annurev.earth.32.101802.120201.

Smith, N.D., and Perez-Arlucea, M., 1994, Fine-grained splay deposition in the avulsion belt of the lower Saskatchewan River, Canada: Journal of Sedimentary Research, v. 64, no. 2b, p. 159–168.

Smith, N.D., Cross, T.A., Dufficy, J.P., and Clough, S.R., 1989, Anatomy of an avulsion: Sedimentology, v. 36, no. 1, p. 1–23, doi:10.1111/j.1365-3091.1989.tb00817.x.

Sonneman, J.A., Sincock, A., Fluin, J., Reid, M., Newall, P., Tibby, J., and Gell, P., 2000, An Illustrated Guide to Common Stream Diatom Species from Temperate Australia: Thurgoona, Cooperative Research Centre for Freshwater Ecology, 166 p.

Stouthamer, E., and Berendsen, H.J.A., 2001, Avulsion frequency, avulsion duration, and interavulsion period of Holocene channel belts in the Rhine-Meuse Delta, The Netherlands: Journal of Sedimentary Research, v. 71, no. 4, p. 589–598, doi:10.1306/112100710589.

Sutherland, R., and Norris, R.J., 1995, Late Quaternary displacement rate, paleoseismicity, and geomorphic evolution of the Alpine fault: Evidence from Hokuri Creek, South Westland, New Zealand: New Zealand Journal of Geology and Geophysics, v. 38, no. 4, p. 419–430, doi:10.1080/00288306.1995.9514669.

Sutherland, R., Berryman, K., and Norris, R.J., 2006, Quaternary slip rate and geomorphology of the Alpine fault: Implications for kinematics and seismic hazard in southwest New Zealand: Geological Society of America Bulletin, v. 118, no. 3/4, p. 464–474, doi:10.1130/B25627.1.

Sutherland, R., Eberhart-Philips, D., Harris, R.A., Stern, T., Beavan, J., Ellis, S., Henrys, S., Cox, S., Norris, R.J., Berryman, K., Townend, J., Bannister, S., Pettinga, J.R., Leitner, B., Wallace, L., Little, T., Cooper, A.F., Yetton, M., and Stirling, M., 2007, Do great earthquakes occur on the Alpine fault in central South Island, New Zealand?, *in* Okaya, D., Stern, T., and Davey, F., eds., A Continental Plate Boundary: Tectonics at South Island, New Zealand: American Geophysical Union Geophysical Monograph 175, p. 235–251, doi:10.1029/175GM12.

Törnqvist, T.E., Wallace, D.J., Storms, J.E.A., Wallinga, J., van Dam, R.L., Blaauw, M., Derksen, M.S., Klerks, C.J.W., Meijneken, C., and Snijders, E.M.A., 2008, Mississippi Delta subsidence primarily caused by compaction of Holocene strata: Nature Geoscience, v. 1, p. 173–176, doi:10.1038/ngeo129.

Troels-Smith, J., 1955, Characterisation of unconsolidated sediments: Danmarks Geologiske Undersøgelse IV, v. 3, p. 1–73.

van Asselen, S., Stouthamer, E., and van Asch, T.W.J., 2009, Effects of peat compaction on delta evolution: A review on processes, responses, measuring and modeling: Earth-Science Reviews, v. 92, p. 35–51, doi:10.1016/j.earscirev.2008.11.001.

Van Dam, H., Mertens, A., and Sinkeldam, J., 1994, A coded checklist and ecological indicator values of freshwater diatoms from the Netherlands: Netherlands Journal of Aquatic Ecology, v. 28, no. 1, p. 117–133, doi:10.1007/BF02334251.

Van De Vijver, B., Frenot, Y., and Beyens, L., 2002, Freshwater diatoms from Ile de la Possession (Crozet Archipelago, Subantarctica), Berlin, Cramer, Bibliotheca Diatomologica, 412 p.

Van Dissen, R., Cousins, J., Robinson, R., and Reyners, M., 1994, The Fiordland earthquake of 10 August 1993: A reconnaissance report covering tectonic setting, peak ground acceleration, and landslide damage: Bulletin of the New Zealand National Society for Earthquake Engineering, v. 27, no. 2, p. 147–154.

Weldon, R.J., Fumal, T.E., Powers, T.J., Pezzopane, S.K., Scharer, K.M., and Hamilton, J.C., 2002, Structure and earthquake offsets on the San Andreas fault at the Wrightwood, California, paleoseismic site: Bulletin of the Seismological Society of America, v. 92, no. 7, p. 2704–2725, doi:10.1785/0120000612.

Weldon, R.J., Scharer, K., Fumal, T., and Biasi, G., 2004, Wrightwood and the earthquake cycle: What a long recurrence record tells us about how faults work: GSA Today, v. 14, no. 9, p. 4–10, doi:10.1130/1052-5173(2004)014<4:WATECW>2.0.CO;2.

Wells, A., and Goff, J., 2007, Coastal dunes in Westland, New Zealand, provide a record of paleoseismic activity on the Alpine fault: Geology, v. 35, no. 8, p. 731–734, doi:10.1130/G23554A.1.

Wells, D.L., and Coppersmith, K.J., 1994, New empirical relationships among magnitude, rupture length, rupture width, rupture area and surface displacement: Bulletin of the Seismological Society of America, v. 84, no. 4, p. 974–1002.

Williams, P.W., King, D.N.T., Zhao, J.-X., and Collerson, K.D., 2004, Speleothem master chronologies: Combined Holocene ^{18}O and ^{13}C records from the North Island of New Zealand and their palaeoenvironmental interpretation: The Holocene, v. 14, no. 2, p. 194–208, doi:10.1191/0959683604hl676rp.

Wilmshurst, J.M., McGlone, M.S., and Charman, D.J., 2002, Holocene vegetation and climate change in southern New Zealand: Linkages between forest composition and quantitative surface moisture reconstructions from an ombrogenous bog: Journal of Quaternary Science, v. 17, no. 7, p. 653–666, doi:10.1002/jqs.689.

Yanites, B.J., Tucker, G.E., Mueller, K.J., and Chen, Y.-G., 2010, How rivers react to large earthquakes: Evidence from central Taiwan: Geology, v. 38, no. 7, p. 639–642, doi:10.1130/G30883.1.

Yetton, M., and Wells, A., 2010, Earthquake rupture history of the Alpine fault over the last 500 years, *in* Williams, A.L., Pinches, G.M., Chin, C.Y., McMorran, T.J., and Massey, C.I., eds., Geologically Active: Proceedings of 11th International Association for Engineering Geology and the Environment Congress, Auckland, September 2010: Boca Raton, CRC Press, p. 881–891.

Science Editor: Christian Koeberl
Associate Editors: John C. Gosse, Jon Pelletier

Manuscript Received 8 March 2012
Revised Manuscript Received 20 July 2012
Manuscript Accepted 10 December 2012

Printed in the USA